REPUBLIQUE ALGERIENNE DEMOCRATIQUE ET POPULAIRE

MINISTERE DE L'ENSEIGNEMENT SUPERIEUR ET DE LARECHERCHE SCIENTIFIQUE

UNIVERSITE DE BLIDA 01

Institut d'Aéronautique et des Etudes Spatiales de Blida

MEMOIRE DE FIN D'ETUDES

Pour l'obtention du diplôme Master en Aèronautique

Option : Propulsion avion

THEME :

SIMULATION NUMERIQUE D'UN ECOULEMENT DANS UNE ROUE D'UN COMPRESSEUR CENTRIFUGE

Réalisé par :

SI MOHAMMED LIZA

BENBACHIR RADIA

-Mr. Sbaa LAZAB **Encadreur**

-Mr.Rachid RENAN **Co-Encadreur**

Blida, 2020

PEOPLE'S DEMOCRATIC REPUBLIC OF ALGERIA

MINISTRY OF HIGHER EDUCATION AND SCIENTIFIC RESEARCH

SAÂD DAHLEB Blida 01 University Faculty of Technology

Institute of Aeronautics and Space Studies

THESIS

In Partial Fulfillment of the Requirements for the Degree of Master in Aeronautics

Specialty: Propulsion

NUMERICAL SIMULATION OF A FLOW IN A WHEEL OF A CENTRIFUGAL COMPRESSOR

Made by:

SI MOHAMMED LIZA

BENBACHIR RADIA

- Mr. Sbaa LAZAB — Advisor

- Mr.Rachid RENAN — Vice-Advisor

Blida,2020

Abstract :

This work is a numerical investigation in three dimensions of the unsteady flow in a centrifugal compressor wheel, which it shows the influence of the mass flow rate and rotational speed on its performances. The study was based on examining the impact of their modeling on the prediction of the flow in centrifugal compressors. It was performed under a viscous turbulent aerodynamic approach using the(KW SST) model, we end this by a validation with another turbulent model (k-ϵ) in light of the comparison.

Key word: Centrifugal compressor, , aerodynamics, turbulence ,numerical investigation.

Résumé:

Ce travail est une investigation numérique en trois dimensions de l'écoulement instable dans une roue de compresseur centrifuge, qu'il montre l'influence du débit massique et de la vitesse de rotation sur ses performances. L'étude est basée sur l'examen de l'impact de leur modélisation sur la prédiction du débit dans les compresseurs centrifuges. Elle a été réalisée selon une approche aérodynamique turbulente visqueuse en utilisant le modèle (KW SST), nous terminons cela par une validation avec un autre modèle turbulent (k-ϵ) à la lumière de la comparaison.

Mot clé : Compresseur centrifuge, , aérodynamique, turbulence , investigation numérique

ملخص :

هذا العمل هو تحقيق رقمي ثلاثي الأبعاد للتدفق غيرالمستقر في عجلة ضاغط طرد مركزي ، مما يوضح تأثير تدفق الكتلةوسرعة الدوران على أدائها. تستند الدراسة إلى فحص تأثير نمذجتهم على التنبؤ بالتدفق في ضواغط الطرد المركزي. تم إجراؤه باستخدام نهج ديناميكي هوائي مضطرب لزج باستخدام النموذج (KW SST) ، وننهي ذلك بالتحقق من صحة نموذج مضطرب آخر (k-ϵ) في ضوء المقارنة.

كلمات مفتاحيه : الكلمات الرئيسية: ضاغط الطرد المركزي ، الديناميكا الهوائية ، الاضطراب ، التحقيق الرقمي

Acknowledgment

At the end of this work, I address my thanks firstly to God Almighty for the power, health and patience that he gave me during all these long years of study. I thank you very much my promoter, LAZAB SBAA who helped me and being with me during my work, who Taught me all what I need not what I want and make me learn from my mistakes by his precious advice and teach me how can I link between reality and simulation on pc by understanding the phenomenon. I would also like to thank my vice promoter Mr. RENAN Rachid who guided me while I'm working by making the hardest steps easier. Without his passionate participation and input, the validation survey could not have been successfully conducted, also I wanted to thank Mr. AOUDA ZOUAOUI in particular to all the amount of knowledge he taught us.

Finally, I must express my very profound gratitude to my sister and binomial without her I could never be here, providing me with unfailing support and continuous encouragement throughout my years of study and through the process of researching and writing this thesis. This accomplishment would not have been possible without them. Thank you.

SI MOHAMMED LIZA

BEN BACHIR RADIA

Dedication

In the Name of Allah, the Most Merciful, and Prayers and peace be upon Mohamed His servant and messenger.

I dedicate my dissertation work to my family and many friends. A special feeling of gratitude to my loving parents, whose words of encouragement and push for tenacity ring in my ears.

My special brothers that have never left my side making the process way easier. I also dedicate this dissertation wholeheartedly tofor their generous support they provided me throughout my entire life and particularly through the process of pursuing the master degree. Because of their unconditional love and prayers, I have the chance to complete this thesis

I dedicate this work and give special thanks to my best friendsLIZA and ryma,to my dearest friends for being there for me throughout my entire lifesouad ,Selma, hiba , ran ,wissem,hayat and hakima,aicha,assia. All of you have been my best cheerleaders.

To all the people in my life who touch my heart, I dedicate this research

إهداء

ها أنا ذا أختم بحث تخرجي بكل همة لاقف عند نهاية المسير وأمتن لكل من كان له فضل في مسيرتي، وساعني ولو باليسير..

فمن اتقى الله تعالى وملأ الإخلاص قلبه، وعلم الله منه صدق نيته، وأكثر من دعائه، فقد أخذ بمجامع الأسباب الموصلة إلى التوفيق، فالحمد لله دائما و ابدا

الى احن قلب قام باحتوائي و كان اول سند لي و عمر حبهما قلبي (جدي و جدتي) اسكنهما الله فسيح جناته

إلى من أفضلها على نفسي ولم لا فلقد ضحت من أجلي، ولم تدخر جهداً في سبيل إسعادي على الدوام (أمي الحبيبة).

الى صاحب الوجه الطيب والأفعال الحسنة، فلم يبخل علي طيلة حياته (والدي العزيز).

الى سندي و ملاذي و من علمني حب الحياة (اخوتي)

يا من سعيتم على نجاحي و حرصتم على بلوغي خط النهاية بكل همة و فلاح استاذتي عائشة و معلمتي آسيا و رفيدة شكر الله سعيكم

الى من تحلو بالاخاء و التميز و الوفاء و العطاء و كانو رفقة لي في هاذا المشوار الطيب (هبة .. رادية و رانية)

إلى زملائي وجميع من وقفوا بجواري وساعدوني بكل ما يملكون وفي أصعدة كثيرة(أمير الياس سارة يقين نجيب أمينة رزيقة سلمى و سفيرات القرآن)

إلى قطتي الجميلة مينا التي سهرت معي الليالي اثناء ساعات بحثي لإنجاز هذه المذكرة

أقدم لكم هذا البحث وأتمنى أن يحوز على رضاكم

الطالبة: ليزة سي محمد

TABLE OF CONTENTS

List of symbols :

ġ :Heatquantity

$P_{i(i=1,2,3)}$: Static pressure

$P_{ti(i=1,2,3)}$: Total pressure.

$T_{i(i=1,2,3)}$,T_{is}:Static temperature.

$T_{ti(i=1,2,3)}$:Total temperature.

$\overrightarrow{w}$,$\vec{T}$: Shaft torque .

$\vec{c}$:Fluid velocity vector.

$Plage$: Rang of work of a compressor

$Marge$: Surge margin

C_P : Specific heat at constant pressure.

S : Entropy.

η_{is-tt} : Total isentropic efficiency.

N, Ω : Rotational speed.

C_{m1} : Axial speed at the entrance of the mobile wheel.

U_2:Training speed.

$\rho_{i(i=1,2,3)}$: Density.

Pr_t :Turbulent Prandtl number

g_i:Component of the gravitational vector in the i direction

v : Control volume

μ_t:Turbulent viscosity

S_1 : Meridian plane.

S_2 : Blade-to-dawn plane.

SS : Suction side of the blade.

PS : Pressure side of the blade.

y^+ : Dimensionless distance to the wall.

u+ : Reduced speed.

U_r: Reduced speed : Speed of friction with the wall.

Δy: Thickness of the boundary layer.

R_{eL} : Reynolds number.

F_d : Distortion factor.

DNS : Direct Numerical Simulation.

LES: Large Scale Simulation or Large Eddy Simulation.

RNG: The statistical approach or Reynolds Averaged Navier-Stokes.

$\overline{P}$: Average pressure.

K:Turbulent kinetic energy.

ε : Turbulent dissipation.

SST:Transport shear stress.

C_D: Flow blocking coefficient.

A_1 : Passage section at the impeller inlet.

r_{tip} : The royen tip.

r_{hip} : The royen hip.

$M_{abs(i),(i=1,2,3)}$: Absolute Mach number.

$M_{rel(i),(i=1,2,3)}$: Relative Mach number.

$\dot{m}_{i(i=1,2,3)}$: Air flow rate.

$W_{u(i),i=1,2,3)}$: Tangential relative speed.

$C_{(i)}$: Absolute speed.

b_3 : The height of the vane at the outlet of the diffuser.

$\sigma_{s(i)}$: Slip coefficient.

R : Particular gas constant.

W_P: Frictional energy.

$Span$: The wingspan.

W:Relative speed.

F : External forces.

R_{i-c} : Richardson's number due to curvature.

$R_{i-\Omega}$: Richardson's number due to rotation.

I:Rothalpy.

h:Enthalpy.

R_m:Meridian radius.

V_{wake}:Absolute velocity of wake flow.

V_{slip}:Absolute velocity of the slipstream.

W_{wake}: The relative velocity of the wake flow.

(Z, R): The 2D plane marker.

C_{u1}: Absolute tangential velocity.

d/dt: The derivative with respect to time.

$\partial/\partial t$: The Local Derivative.

σ: Angle.

α_{blade} : The geometric angle at the exit of the diffuser.

σij : Viscous stress tensor.

σk : The Closing Coefficient.

σt : The Constant Total Pressure Drop Coefficient.

σε : The Closing Coefficient, constant.

σω : The Closing Coefficient, constant.

τij: Reynolds Stress Tensor.

τ : Stress Tensor

$\delta_{m,c}$: Boundary layer thickness (m: hub; c: housing).

$\delta_{+,-}$: Boundary layer thickness (+ : the extrados ; - : the intrados).

$\gamma = Cp / Cv$: The Dimensionless Heat Ratio Coefficient for specific heat.

μ: Dynamic Viscosity

υ: Kinematic Viscosity

α_1:The absolute angle at the rotor inlet.

α_2:The absolute angle at the exit of the rotor.

β_1:The relative angle of the flow at the rotor inlet.

β_2:The relative angle of the flow at the rotor outlet.

π_c:The pressure ratio between the outlet and inlet of the compressor.

Ψ: Pressure Coefficient .

ϕ : Air flow coefficient

LIST OF FIGURES:

CHAPTER I

CHAPTER 2

CHAPTER 3

CHAPTER 4

LIST OF TABLES

CHAPTER II

Chapter IV

INTRODUCTION:

Turbochargers are widely used in turbo machinery, especially in the aviation industry as a means of increasing power. The most commonly used are those with radial compressors because of their ability to absorb more power and give a high pressure ratio at low airflow compared to axial turbochargers of the same size.

A centrifugal compressor stage is composed of two parts, a moving part (centrifugal impeller), the main role of this impeller serves to increase the energy of the fluid both in the form of heat and stop pressure, this increase in stop pressure is broken down into an increase in static pressure also an increase in kinetic energy. The other fixed part is the diffuser, the role of this part is to decrease the stopping pressure due to losses, on the other hand, the transformation of the form of energy has an increase in static pressure and decrease in kinetic energy.

The analysis of the flow in this compressor wheel generally, three-dimensional flow, compressible, viscous and turbulent. Therefore, to treat this problem analytically difficult to solve, but numerically possible, for this we use the software ANSYS CFX This software consists of three models, the first model is the special CFX -Blade Gen for 3D generation of the surveyor, the second CFX-Turbogrid for generation of structural meshes, the third model is a result processing station.

This work is divided into four chapters :

- The bibliographical analysis allows an understanding of the studied phenomenon by citing some study results.
- The first chapter: presents generalities on turbomachinery and general definitions concerning centrifugal compressors, their classification followed by a description of the different characteristics and internal flows. After having exposed the aerodynamic forces and the general equations governing these flows, and having also exposed the interactions of the flow between rotor-stator.
- The second chapter: presents the method known as the calculation of aerothermodynamic parameters in a centrifugal compressor stage following the one-dimensional analysis method with the assumptions of the calculations, it also calculates different aerodynamic coefficients and losses in this compressor.
- The third chapter: in this chapter deals with numerical modeling and presentation of the software using ANSYS CFX . The modeling of the geometries of the centrifugal compressor wheel has been described in detail and the meshing according to

conditions has been created. In presenting the turbulence plus models, we use in this study (K-w SST). And the finite volume method with numerical discretization, the equations of this problem following a scheme in CFD and the diagrams available in this software.

- The fourth chapter: the results are present for the centrifugal compressor impeller in nominal point; and the validation of the results with the comparison of the numerical results And also, the validation by the comparison of the results with Guillaume DUFOUR's these[4]. And also, the validation by qualitative comparison with the other works.

Finally a conclusion with proposed perspectives for future research.

BIBLIOGRAPHIC REFERENCES

INTRODUCTION:

The flow in a centrifugal compressor is generally viscous and turbulent, three-dimensional, in stationary and compressible fluid.For the study and analysis of the flow in this compressor can be done following by two methods, the numerical method and the experimental method.The numerical method based on the discretization of the basic equations in fluid mechanics to solve the problem, it requires a certain number of simplifications on the quest system.

The experimental method that requires several systems for measurements (pressure, speed, temperature, ...etc). Using visualization techniques for the analysis of different structures of the flow.

Many art researchers already made the study and analyzed the flow in a centrifugal compressor.

D. Eckardt, 1975, analyzes the compressible flow in a centrifugal compressor by experimental study and shows that the flow through the rotor is often divided into two regions at the outlet of the so-called jet and the wake.

Jeske.H ;O .Tepel1983, They used a numerical method to analyze the transonic flow in the diffuser of a high pressure ratio centrifugal compressor, and determine the boundary layer flow over the length of the blades and also calculate the pressure distribution two-dimensional to the hub by the numerical method of finite differences and to make the comparison with results the experimental one.

Alain Berlioz1991 , established an efficient method for calculating rotating industrial structures such as pump wheels, centrifugal compressors. . . Such structures are characterized by complex geometries and conventional finite element analysis leads to models with a large number of degrees of freedom. He presented in detail the establishment of the theoretical model adapted to cyclic symmetry structures subjected to centrifugal effects. The method is first validated on simple representative examples, then applied to an industrial structure. Frequencies and modes are experimentally determined when stopped and rotated in an over-speed pit under partial vacuum. The theoretical results are then compared to the experimental results. A very satisfactory concordance is obtained.

Michal .D ; Hathaway ; Randall M.chriss ; Jerry R.Woodet Anthony J ; Stragisar 1993: In NASA, they analyzed the flow in a low speed centrifugal compressor and used both numerical and experimental methods.

W. N. Dawes 1995 et ceux de O. Domercq et R. Thomas, 1997.They used both numerical and experimental methods to analyze the flow in a stage of a centrifugal compressor and they demonstrate that the diffuser can have a significant influence on the flow that develops in the centrifugal wheel.

CharlooteBarbier2002,[3]He made the numerical and experimental study the flow in a centrifugal compressor based on the interaction between Rotor and Stator. Numerically, it uses the CoLIBRI calculation code in stationary regime, and the experimental study requires measurements by LASER using a L2F velocimetry between the centrifugal wheel and radial diffuser, and it makes the comparison between the two methods.

Guillaume DUFOUR 2006,[4]Compared the CFD results with experimental data available on two configurations, one called academic and the other from the industrial database by applying the laws of similarity of reynolds to show the contribution of numerical modeling in the design centrifugal compressors, such a concept allows to consider the design of new machines based on a database of etages.

Jan van Helvoirt2007, Jan van Helvoirt deals with low-frequency pulsation phenomena in full-scale centrifugal compression systems associated with compressor surge. The Greitzer lumped parameter model is applied to describe the dynamic behavior of an industrial compressor test rig and experimental evidence is provided for the presence of acoustic pulsations in the compression system under study. It is argued that these acoustic phenomena are common for full-scale compression systems where pipe system dynamics have a significant influence on the overall system behavior.

J.Lig ; K.C.Wong et S.Armfiell2007,They numerically study a small three-dimensional centrifugal compressor and using ansyscfx 5 software to determine compressor performance, using the K-Omega, SST turbulence models for 10e-4 convergence order.

Nicolas Rochuon, 2007,The study concerns a centrifugal compressor designed by Turbomeca. His design breaks with conventional compressor designs by introducing a non-axi-symmetric hub wheel. An experimental and numerical approach is proposed for flow analysis in this type of configuration. First, the study shows the ability of the new design to

modify the flow structure in the moving wheel. In the present case, the beneficial effect of a reduction in vorticity is counterbalanced by an increase in crankcase losses by shearing. Secondly, an analytical treatment of the experimental and numerical results makes it possible to quantify the purely unsteady contribution of the rotor-stator interaction. The analysis shows in particular that the periodic modification of the shock structure attached to the diffuser is at the origin of a significant increase in losses, compared to those predicted by stationary simulations.

Elnashar, H. Amr 2008,Did a test rig built for determining a centrifugal compressor impeller flow field characteristic parameters whereas, the impeller efficiency, slip factor and aerodynamic blockage were calculated at every measured point he developed a loss model using the basic fluid equations aided by some empirical relations, then it was applied on the measured cases. An aerodynamic 3-D viscous flow analysis was made using "CFX-BladeGen" softwarepackage. A comparison between measured and theoretically calculated results showed a good agreement.

Michel TOUSSAINT 2011,[3] he studied experimentally the behavior of a centrifugal compressor at low revs vis-à-vis the phenomenon of pumping in unsteady conditions where the risk is very real

MAAMMEUR Moustafa 2011,performed a numerical investigation into the three-fold flow dimensions in a centrifugal compressor, which shows the affection of the performances by two geometrical parameters, the angle β2 at the outlet and the section at the inlet of the centrifugal compressor. The study is made according to an aerodynamic approach in turbulent regime but also in thermodynamic approach in order to compare them.

BENREZZAK SAMIR 2012,In his thesis, he carried out the study of a centrifugal compressor of the Oued-Noumer station. He realized for this calculation verification thermodynamics of the performance of the centrifugal compressor k101A and a mechanical calculation of this compressor. And also addressed the problem that influences the functioning of the Centrifugal compressor k101A due to wear of the components until failure.

LAAZAB Sbaa 2013,[1]did a numericalsimulation of a turbulent unsteady flow in a centrifugal compressor stage and compared the obtained results with an experimental one.

AurélienMarsan2013,Carried out a study that fits in the context of the control of flows in turbomachines. Following the proven interest of the suction of the boundary layer in axial

compressors to improve performance. The study aims to evaluate if this control methodology is relevant in radial geometry. It relies for this on a Turbomechanicaltranssonic centrifugal compressor.

Paul Le Sausse2014, created a numerical model to simulate the flow in this type of compressor. In order to meet industrial requirements, a first geometry has been established by iterative modifications of various parameters and analysis of the induced performances. The flow was then studied more precisely, particularly to better understand the occurrence of detachments. Finally, an unsteady study of the flow in the diffuser was carried out. Beyond the physical phenomena studied and apprehended during this process, it is above all a methodology that values this work.

Patricio ALMEIDA,2014 presented a simulation of contact dawn-crankcase, with a model of bladed wheel in contact with a crankcase, The influence of each physics on the dynamic behavior The contributions of this work are mainly experimental, in terms of the multi-dimensional spectral analysis of the measurements and on the phenomenological level. this simplified model validates the experimental hypotheses and confirms that Sidebands can be the cause of undesirable behavior in turbomachines.

YannickBousquet 2014, he investigated the mechanisms responsible for the loss of stability of a centrifugal compression stage. The underlying industrial goal is to expand the compressor's stable operating range. The work is approached numerically using the elsA calculation code, developed by ONERA and CERFACS. Unsteady simulations are performed on the complete circumference of the wheels. The topology of the flow is first analyzed according to three stable operating points distributed over the characteristic curve of the design iso-speed. This analysis makes it possible to describe the evolution of phenomena when the flow rate is reduced. In the vicinity of the stability line, the excessive incidence on the rotor blades triggers the delamination of the boundary layer on the face in expression.

Stefan UbbenReinhardNiehuis J. Turbomach. Mar 2015 did an experimental Investigation on the influence of the diffuser clearance on the operating behaviour of an entire stage of a centrifugal compressor, the pressure recovery in the diffuser, and on the diffuser flow by a systematic variation of the parameters , height, vaneangle, radial gap between impeller exit and diffuser inlet, and rotor speed. Compressor map measurements provide a summary of the operating behaviour related to diffuser geometry and impeller speed. The results presented show that an one-sided diffuser clearance does not necessarily has a negative

impact on the operation and loss behavior of the centrifugal compressor, but instead may contribute to an increased pressure ratio and improved efficiency.

Van thang Nguyen 2016, determined the effect of rotor-rotor aerodynamic interaction on compressor performance. In addition, the experiment to realize the characteristic of the counter-rotating compressor near the pumping to evaluate the adaptaion of the compressor with low mass flow.

Aleksey Yablokov ,died in Moscow, Russia, on Jan. 9, 2017did a CFD numerical simulation using ansys CFX on a centrifugal compressor stages with low flow rate coefficient (F=0.028) estimated discrepancy between the results of numerical researches on the model with shaft seal labyrinth and without shaft seal labyrinth . the solution used a second order discretization scheme maximum value of residual in calculation parameters is 10e-5.

Elias Sundstrom, 2017,Employed an LES approach with the purpose to predict the unsteady flow field in a ported shroud centrifugal compressor equipped with a vaneless diffuser, direct comparison has been possible in terms of global performance parameters but also in terms of flow variables. He found that computed results are in good overall agreement with measured data for a range of operating conditions.

Victor Moënne-Loccoz2019, did an experimental study on characterization of aerodynamic instabilities developing in a centrifugal compressor and a first evaluation of the effectiveness of a boundary layer suction control strategy. The compressor, developed by Safran Helicopter Engines and called Turbocel, is composed of an input steer wheel, a split centrifugal wheel, a split and split radial diffuser and an axial straightener. Previous digital work done at the Laboratory of Fluid Mechanics and Acoustics have shown, at low rotational speeds, a singular behavior characterized by an "alternating" flow structure involving two adjacent channels of the radial diffuser.

PavelSitkin, 2019,Studied the improvement of the design procedure for the volute of centrifugal compressors based on verification of the volute calculation data obtained with the Solidworks software package with experimental data using the finite-difference elements method.

Andrzej Tomasz Jerzak,[5]provided new results in the field on adaptive control of surge in axial andcentrifugal compressors, two types of surge actuators are being studied: closed coupled valve (CCV) and a piston. Both actuators were previously operated by standard P-controllers for which the gains can be constructed by the coefficients from the compressor map .The results through simulations showed that this methodology had rather poor accuracy or at least requires a comprehensive amount of tuning. Still, the result were considered sufficient for the applications.

CHAPTER 1

GENERALITIES ON TURBOMCHINES

1.1. General definition:

A turbomachine is a device where mechanical energy, in the form of the shaft work, is transferred either to or from a continuously flowing fluid by the dynamic action of rotating blade rows

1.2. Classification:

1.2.1. Function:

- Work absorbing: compressors or fans
- Work producing: turbines

1.2.2. Nature of the fluid :

Compressible / Incompressible: The compressible fluid undergoes variations in its density which must be taken into account especially if they are important. The incompressible fluid undergoes almost no variation in its density .

1.2.3. **Geometry Méridional projection (Z-R):** axial / radial

1.3. Centrifugal compressor:

The centrifugal compressor can be centrifugal or axial then centrifugal, it produces compressed air for combustion, air conditioning, propulsion ... etc. In the centrifugal compressor, high pressure is accomplished to impart kinetic energy to the fluid. Speeds are relatively high and it happens that at such speeds; the compressor suffocates and even reaches the breaking of the blades, this due to the number of Mack(the shock wave), when it approaches the unit, it is an area to avoid. Another phenomenon occurs for the low speeds that it is about surge,

the effect of compressibility is taken into consideration at each point of the compressor. The fluid that passes through the compressor wheel, it gives it energy by communicating a relatively high output speed (subsonic) depending on the desired compression ratio. In a centrifugal compressor, a "spinning wheel" composed of blades draws the air axially and delivers it radically after having accelerated and compressed it, thanks to the effect of the centrifugal force and the rotation speed. This air is then straightened in a fixed blade which transforms a portion of the energy into pressure. A collector recovers this compressed air.
The compressor has the advantage of providing a compression ratio, in a stage higher than that of a 5-stage axial compressor , on the other side its radial size is important.
Compressor type as a function of flow rate and pressure .

Centrifugal compressors are capable of delivering 900 to 35,000 m^3 / h of flow. They are found as soon as the required capacity exceeds 7000 m^3 / h. Above 35,000 m^3/h, axial flow compressors take over.

They are particularly suitable and energy efficient when the demand is relatively constant and high.

Their specific consumption at full load varies between 100 and 125 h / m^3. Among these competitors, axial compressors, reciprocating compressors, screw compressors , the centrifugal compressor is the solution in many situations.

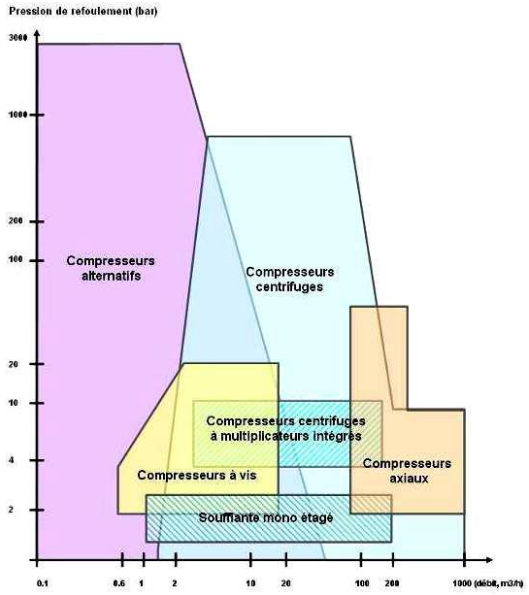

Figure1.1: Compressor type as a function of flow rate and pressure

1.4. Geometry and characteristics:

A centrifugal compressor can be designed in many different ways, c.f. Aungier (2000). For introductory purposes Figure 1.2 provides schematic front and side views of a typical centrifugal compressor stage. Key components are (see also Fig. 1.2): an inlet duct station (0-1), an impeller (1-2), a diffuser (2-3), a volute (4), and finally an outlet duct (5) for flow discharge where the compressed flow may be utilized for some specific purpose.
The impeller energizes the fluid by its rotation (in the clockwise direction in the figure). At the exducer station (2), the flow enters the diffuser. There, additional fluid kinetic energy is recovered before the flow discharges into the volute. In the figure the diffuser is sketched as an empty space, and is commonly referred to as a vane less diffuser design. However, some diffuser designs may be equipped with guide vanes for flow control. Guide vanes may also be present upstream of the inducer (1), commonly denoted as inlet guide vanes. A volute is utilized to smoothly guide or collect the flow towards the exit cone and eventually being funneled out via the outlet duct. The appearance of the volute is very much based on experiences from previous well-functioning designs. A popular choice from a design perspective is to employ a cross-section area variation as function of the tangential direction.

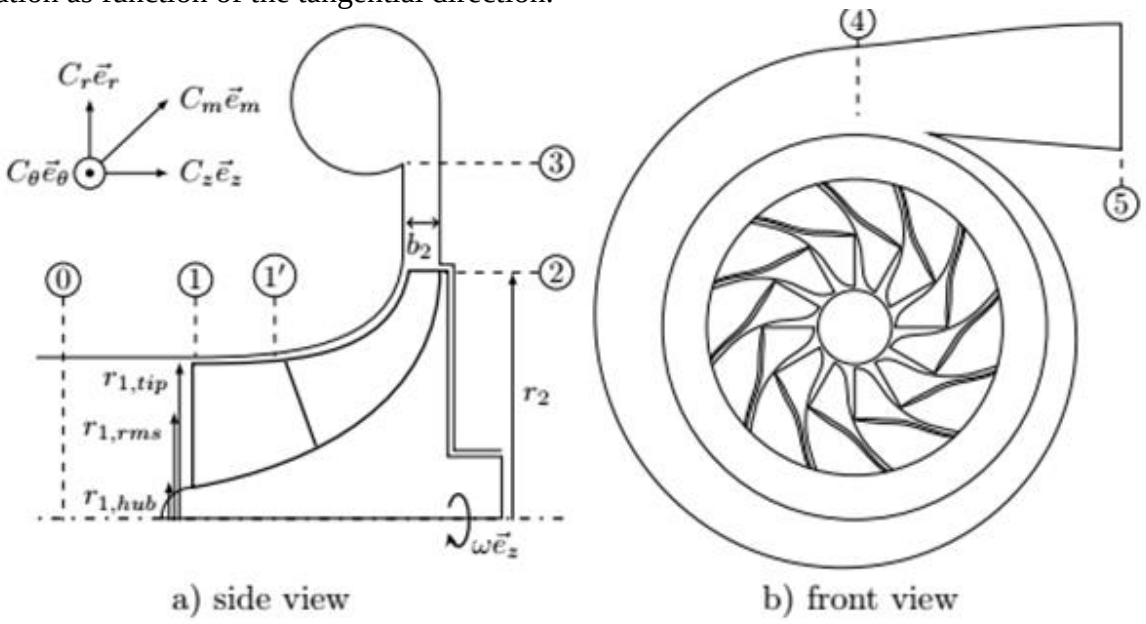

Figure 1.2:side and front view sketches illustrating a typical centrifugal compressor stage

In the sketch a simple spiralfunction was adopted. The figure also depicts an intermediate line a little downstream of the inducer, i.e. station(1), this serves to highlight that some impeller designs incorporates blades with a shorter chord. Those blades are called splitter blades whereas the others are called full length or main blades.
A question is how and why a torque input on the impeller shaft delivers power to the fluid. It is recognized that the compressor is an open system in the sense that fluid can cross the system boundaries at the inlet and the outlet.

Downstream of the inducer, i.e. station (1). This serves to highlight that some impeller designs incorporates blades with a shorter chord. Those blades are called splitter blades whereas the others are called full length or main blades.
A question is how and why a torque input on the impeller shaft delivers power to the fluid. Itis recognized that the compressor is an open system in the sense that fluid can cross the system boundaries at the inlet and the outlet.

From the first law of thermodynamics for a steady flow in such an open system there must be an energy balance. On one side of the balance equation:

$$\dot{w} + \dot{q} = \dot{m}\Delta\left(e + pv + \frac{c^2}{2}\right) \tag{1.1}$$

There is a sum of work done on the system $\dot{w}$ and an input due to heat transfer $\dot{q}$. The work done is due to the rigid body rotation of the impeller wall surface boundary, expressed as the angular velocity of the impeller times the applied shaft torque $\vec{w}$, $\vec{T}$ The heat transfer $\dot{q}$ is an energy flow between the system and its environment due to heating or cooling, which is most often neglected for centrifugal compressors. The equation is balanced on the right hand side with the mass flow rate $\dot{m}$ multiplied with changes in the flow energy consisting of internal energy e, work required $P\ V$ to move the fluid across the system boundaries, and the kinetic energy $C^2/2$, where $\vec{c}$ is the fluid velocity vector. The sum $(e + p)$ is defined as the specific enthalpy h and together with the kinetic energy term it is defined as the total enthalpy $h0$, respectively. Therefore, the appropriate energy equation for a compressor is:

$$\dot{w} = \dot{m}\Delta h_{\circ} = \dot{m}(h_{\circ}d - h_{\circ}i) \tag{1.2}$$

1.5. Theory of centrifugal compressors:

where the energy change is taking place for a compressor operating between inlet total conditions ($p0i$, $T0i$) and discharge ($P0d$, $T0d$). The change in total enthalpy is often normalized with the blade tip speed U which is called the work coefficient[1]

$$\psi = \frac{\Delta h0^2}{U} \tag{1.3}$$

For incompressible flow and using $\Delta h = \Delta p/\rho$it can be put in the followingform:

$$\psi = \Delta p/(\rho U^2) \tag{1.4}$$

Instead of defining a change it is also common to define a pressure increase as a ratio between inlet and discharge:

$$PR = \frac{pd}{pi} \tag{1.5}$$

For a reversible process the specific entropy *s* is defined as:

$$ds = dqrev/T \tag{1.6}$$

The second law of thermodynamics dictates the direction of the compression process from inlet to discharge. For an adiabatic process it requires $\Delta s = 0$. A process that is both adiabatic and reversible is said to be isentropic, i.e. a constant entropy. For a closed system the thermodynamic relation for entropy is:

$$T\,ds = dh - vdp \tag{1.7}$$

Thus, assuming an isentropic process, the work input required to produce the pressure rise would be a little less than the actual $\Delta h0$. This is denoted as:

$$\Delta h_{\circ}s = \int_{i}^{d} vdp \tag{1.8}$$

The *h-s* diagram Figure 1. 3 It consists of two parts, one ideal process (constant entropy) and one isobaric process (constant total pressure). The isobaric curves in Figure 1.3 are obtained from the entropy change *ds* in the fluid:

$$ds = \frac{dh}{T} - \frac{Rdp}{p} \tag{1.9}$$

In the isobaric case *dp*= 0 and integrating we obtain:

$$T_{\circ} = T_{\circ}ref \cdot e\Delta s/cp \Rightarrow h_{\circ} = h_{\circ}ref \cdot e\Delta s/cp \tag{1.10}$$

which gives an explicit relation between the total enthalpy as function of the change in entropy. The difference between the isobaric curves (e.g. $p_{\circ}ds$ and $p_{\circ}d$) is related to the total enthalpy loss or efficiency of the centrifugal compressor (i.e. $\Delta h_{\circ}s$ compared to $\Delta h_{\circ}$). It is commonly defined as the fraction of the ideal over the actual work input

$$\eta s = \frac{\Delta h0s}{\Delta h0} = h_{\circ}i - \frac{h0s}{h0i} - h_{\circ}d \tag{1.11}$$

Since most compressors operate at moderate temperatures (<<1000 K), a calorically perfect gas with constant heat capacities *cv*and *cp*is generally a good approximation. This allow the alternative efficiency form

$$\eta s = \frac{PR_{\circ}^{(\gamma-1)/\gamma}-1}{(Ti/T_{\circ}d)-1} \qquad (1.12)$$

where*γ= cp/cv* is the ratio of specific heats. In order to obtain an overview of centrifugal compressor performance for various operating conditions the pressure ratio and the efficiency quantities can be combined, see Fig.1.3 It is drawn with several pressure ratio (PR) curves as function of the mass flow rate, where each PR curve is given for a specific impeller speed. On top the efficiency is given as contour lines, with higher levels centered along some optimum design operating condition. At very high mass flow rates, the flow may reach sonic speeds in the impeller blade passages, and the flow becomes choked. This is a limiting boundary called stonewall or choke line. On the other side, towards low mass flow rates there is a limiting boundary called surge, which is a flow phenomenon where the compressor flow undergoes large system oscillation. Stable and robust operation is not possible beyond that limit.[2]

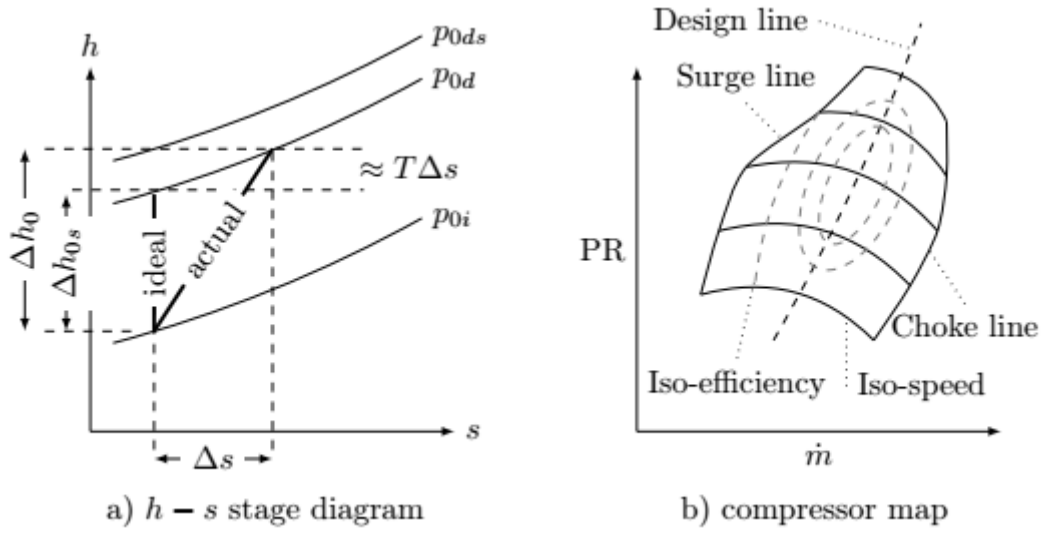

Figure1.3 :schematically drawn stage h-s diagram and compressor map

1.6. Mechanical components of a centrifugal compressor:

Like any mechanical system, the centrifugal compressor consists of some mechanical elements to complete its task. These elements are usually made of aluminum alloy . In what follows, each of these organs will be represented individually.

1.6.1. The upstream part of a compressor:

The upstream part has the role of bringing the flow up to the wheel. In general, we distinguish such diverse elements as: axial pre - rotation valves at the entrance, a plenum supply.

1.6.2. The rotor (wheel):

The wheel is the fundamental element of the compressor, because it ensures the exchange of work, it is indeed the only moving element of the floor. The wheel of Figure 1.4 has what is called an inductive zone, that is to say that the blades start in an axial direction and end in the radial direction.

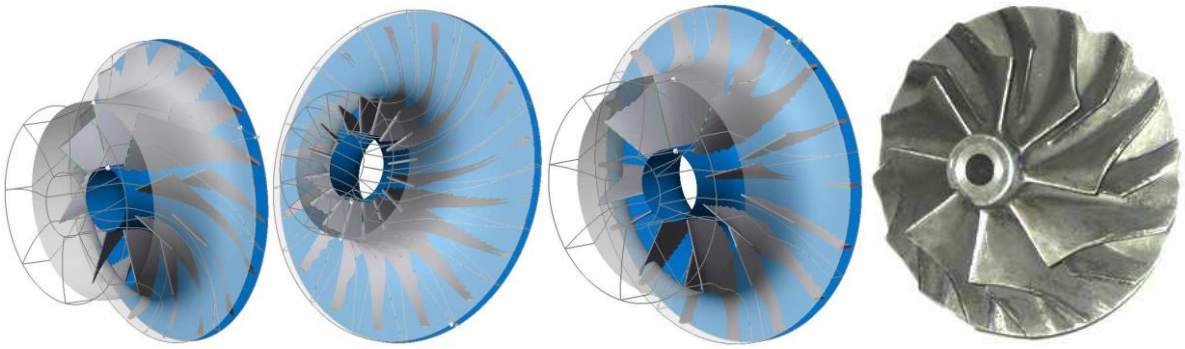

Figure 1.4 : Different shapes of the centrifugal compressor wheel.

The fig 1.4 shows various geometrical shapes of centrifugal compressor wheels . We note in particular the differences between these wheels in terms of the number of blades, the height of the blades and angle of wedging at the exit. The complexity of this type of fully three-dimensional geometry requires the introduction of reference surfaces, which make the flow analysis more accessible. The meridian surfaces are obtained by projection on the plane generating the volume of the wheel; the dawn-to-blade surfaces are generally represented by a transformation according to the average plane and the orthogonal cuts which can be considered as quasi-planar.

There are three types of wheels which differ in the inclination of the blades at their outlet (physical angle of constriction β_2) as shown in the figure 1.5

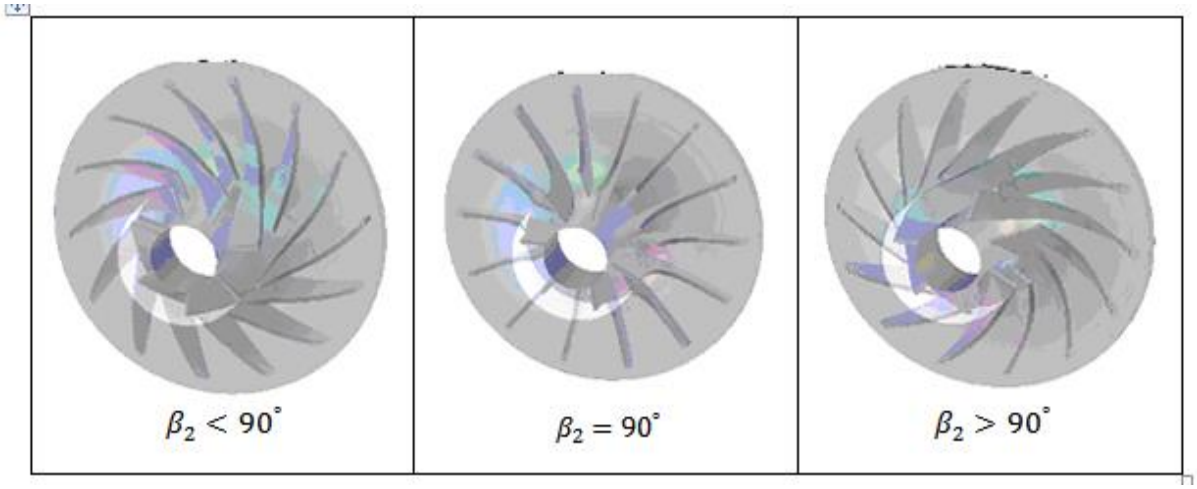

Figure 1.5 The different types of the centrifugal wheels for different angleβ_2

1.6.2.1. Speed triangles for all three cases:

The velocity triangle is a graphical representation of the principle of kinematics according to which the absolute velocity vector ($\vec{C}$)of a fluid particle is composed of the vector of the relative velocity ($\vec{w}$)to the moving wheel plus the linear velocity vector of the moving wheel ($\overrightarrow{U}$)

The figures below represent the triangles of the theoretical velocities at the output of the impeller. [1]

- **Radial balding$\beta_2 = 90^\circ$:**

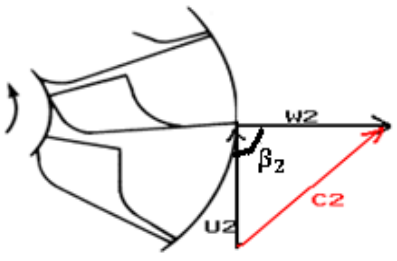

(a)

- **Backward curved blades$\beta_2 < 90^\circ$**

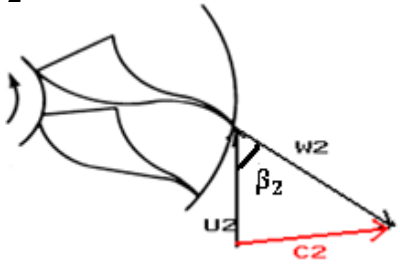

(b)

- **Forward curved blades** $\beta_2 > 90^{\circ}$

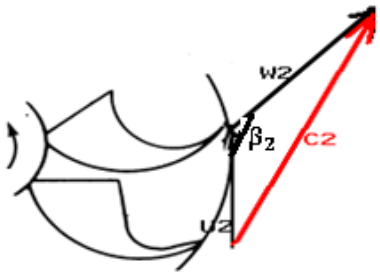

(c)

Figure 1.6: Speed triangles for different blade inclinations

1.6.3. Diffuser:

At the exit of the rotor, the static pressure of the flow increases, but a part of the total pressure brought by the wheel is present in the form of kinetic energy. The role of the diffuser is then to slow down this flow, fig 1.7 because the losses in the downstream conduits strongly depend on the Mach number of the flow. This slowdown also makes it possible to convert part of the kinetic energy into static pressure energy

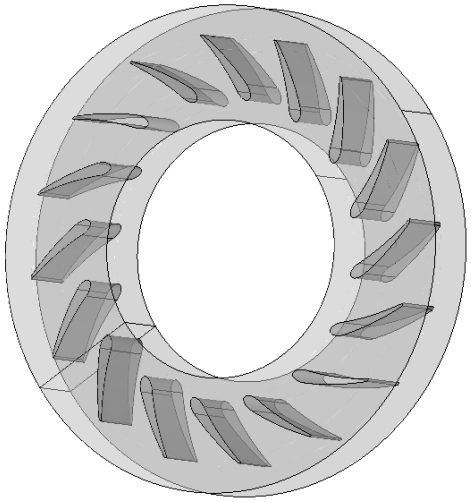

Figure1.7 : Radial diffuser of a centrifugal compressor.

1.6.4. The volute:

The main role of the volute is to collect the radial flow at the outlet of the diffuser, to restore it to the system through a tubular conduit, through an evolution of the passage section. The flow in the volute is often modeled (incompressible fluid hypothesis) by

logarithmic spirals, but a part of the fluid performs the complete gyration and is juxtaposed to the main flow at the beak (zone of beginning of the spiral), Fixed pitch If the wheel is rotating, it gives a flow at the outlet, the air is then collected by volute , or by a system that changes the direction along the axis of rotation for the case ofthe turbojet.

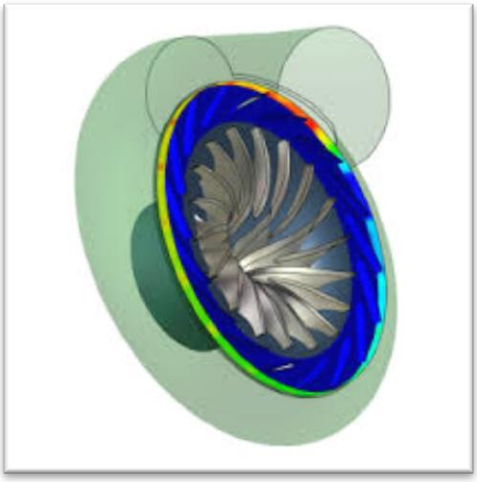

Figure1.8 :the volute

1.7. The different characteristics of a compressor :

Isentropic compression performance Its expression is obtained from the law of the first principle of thermodynamics , the energy equation expressed with the enthalpy in the moving wheel :

Adiabatic transformation case : no change of isentropic temperature, and reversible between position 1 and 2 for a perfect gas therefore

$$dh_t = dq + dw_T \tag{1.13}$$

With:

$$dh_t = c_p \cdot dT_t = \frac{1}{\rho_t} \cdot dp_t + T_t \cdot ds \tag{1.14}$$

$$w_{T1-2} = c_p \cdot (T_{t2} - T_{t1}) = c_p \cdot T_{t1} \cdot (\frac{T_{t2}}{T_{t1}} - 1) = c_p \cdot T_{t1} \cdot \left(\left(\frac{p_{t2}}{p_{t1}} \right)^{\gamma-1/\gamma} - 1 \right) \tag{1.15}$$

$$w_{T1-2} = c_p \cdot T_{t1} \cdot (\pi_t^{\gamma-1/\gamma} - 1) \tag{1.16}$$

If:

- $\pi > 1 \Rightarrow T_{t2} - T_{t1} > 0 \Rightarrow w_{T1-2} > 0$ The work is communicated to the fluid.
- $\pi < 1 \Rightarrow T_{t2} - T_{t1} < 0 \Rightarrow w_{T1-2} < 0$ The work is transmitted by the fluid on the outside

The isentropic efficiency can be defined by the ratio of change in total entropy in isentropic transformation on the variation of actual total entropy :

$$\eta_{isc} = \frac{h_{t2is} - h_{t1}}{h_{t2} - h_{t1}} = \frac{h_{t3is} - h_{t1}}{h_{t3} - h_{t1}} = \frac{T_{2is} - T_{t1}}{T_{t2} - T_{t1}} = \frac{\pi_{c-t}^{\frac{\gamma-1}{\gamma}} - 1}{\tau_t - 1} \quad (1.17)$$

Such as : $\begin{cases} \tau_t = \dfrac{T_{t2}}{T_{t1}} \\ \pi_t = \dfrac{p_{t2}}{P_{t1}} \end{cases}$

transformation is isentropic :

$$\tau_t = \pi_{c-t}^{\gamma-1/\gamma} \quad (1.18)$$

1.8. The compressor field curve :

It is a representation of the pressure rate placed on the ordinate axis as a function of the air flow on the abscissa axis for different speeds of rotation. It is represented by a useful operating zone, limited by a pumping line beyond which the compressor enters pumping or rotating stall and a locking line where the mass flow rate can not increase.

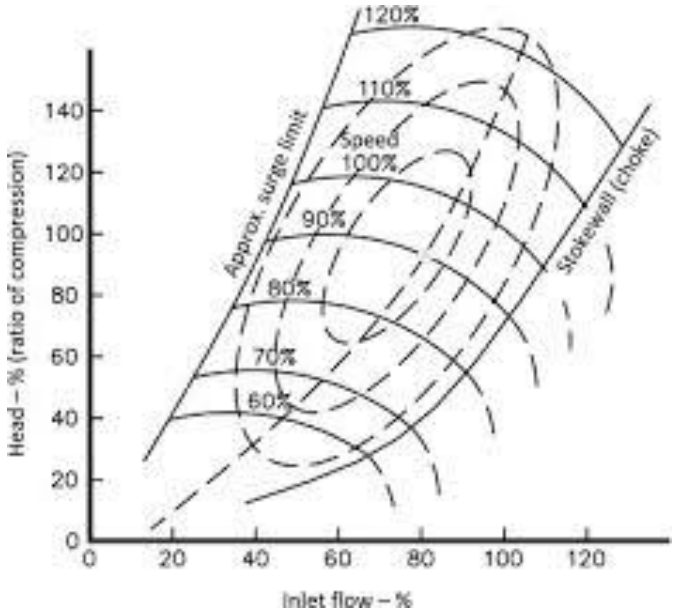

Figure1.9: Characteristic curve of a compressor[3]

So the compression ratio and the efficiency are the main measurements of the performance of a compressor. For the evaluation of this performance we can define :

1.8.1. Origin of the surge line :

The surge line represents the limit to which the compressor cannot operate in a steady state. It passes near the point where t the pressure is maximum.

To determine this line, two coefficients are used:

Coefficient of pressure: $\psi = \frac{\Delta P}{\frac{1}{2}\cdot\rho\cdot U_2^2}$ (1.19)

Flow coefficient: $\phi = \frac{C_m}{U_2}$ (1.20)

The quantities relative to the point of appearance of the pumping are noted :

Flow Retention : $\frac{Q_S}{\varphi_S \cdot S} = \rho \cdot U_2$ (1.21)

Pressure rate : $\left(\frac{P_2}{P_1}\right)_S = \frac{P_1 + \Delta P_S}{P_1}$ (1.22)

From the equation (1.21)we find :

$$U_2 = \frac{Q_S}{\varphi_S \cdot S \cdot \rho} \quad (1.23)$$

Replacing the equation (1.23) in (1.20) and compared ant with (1.22) :

$$\left(\frac{P_2}{P_1}\right)_S - 1 = \frac{1}{2\cdot\rho\cdot S^2\cdot P_1} \cdot \left(\frac{\psi_s}{\varphi_s^2}\right) \cdot Q_S^2 \quad (1.24)$$

The surge line therefore has the appearance of a parabola intersecting the ordinate axis at " 1 " and the abscissa axis at " 0 ". When the speed of rotation of the compressor varies, it is essential that the operating point kept away from this area.

The flow $\varphi_s$is difficult to estimate, and the builders are therefore committed to defining significant margins. The pumping margin can be defined by the following relationship : (1. 24)

$$Marge = \frac{\left(\frac{P_2}{P_1}\right)_S - \left(\frac{P_2}{P_1}\right)_{Dp}}{\left(\frac{P_2}{P_1}\right)_{Dp}} \quad (1.25)$$

The surge margin can reach 10% for centrifugal compressors.

1.8.2. The surge:

The surge is a cyclical form of instability with the symptoms of large amplitude fluctuations both in pressure rise and mass flow in annulus (or duct). If not handled properly, thiscondition may further develop to deep surge where one may experience flow reversal .

The surge cycle, which generates the oscillations.

Initially, the compressor operates at steady-state in the stable area of the compressor. Then, a disturbance is applied on the system resulting in a flow deceleration. The compressor isnow forced to operate at unstable point (1). The flow continues to decrease until it reachesits lower limit at point (2) where the flow now have a negative value and thus becomes reversal. Next, the flow accelerates first to point (3) (where it reaches a zero value) and thento (4) at the stable area. With no changes in the system, the cycle follows the compressorcharacteristic up to the point (1), meaning that the surge cycle repeats.

When the compressor is suffering from some local aerodynamic instability, say rotatingstall, it will be unable to deliver sufficient pressure so that the flow moving downstreamfrom the compressor will lose its continuous nature. This results in the incident of surge.

Seen from other perceptive, the surge is a consequence of the compressor ,which is limitedto constant impeller speed, not keeping up with the excessive increase in system resistancesuch as decrease in throttle opening. The resistance will then reduce the flow, making it reversal and thus unsteady. The unsteady flow will interfere with other componentsbesides the compressor, making the system unstable as a whole. As stated earlier, therotating stall is often viewed as the inception of surge. Ironically, while the flow in purerotating stall is known for its no uniform mass deficit the flow will retrieve its uniformity during the surge condition.*[5]*

A phenomena of surge can be divided into four different types:

- Mild surge: exhibits small pressure oscillations. No evidence of flow reversal.
- Classic surge: will often have larger oscillations at lover frequency then mild surge. Still no flow reversal.
- Modified surge: characterized by unsteady and non-ax symmetric flow. Combination of rotating stall and classic surge.
- Deep surge: a most severe form for surge. Flow reversals are typical. The cycledescribed above occurs for deep surge.

1.8.3. The blocking:

We can observe on the curve of characteristic a slope almost vertical which corresponds to a maximum flow (sonic blocking), but physically if one increases the flow rate of incidence of relative speed will decrease until a minimum value, that corresponds to a obstruction of the channel in which the fluid reaches the speed of sound.

- **The operating range:**

The range of works of a compressor is important , it can be defined e by the following relationship :

$$Plage = \frac{\dot{m}_{blocage} - \dot{m}_{pompage}}{\dot{m}_{nominal}} \quad (1.26)$$

- **The tipping away:**

The rotational detachment can be defined by the formation in the inter-vane channels of variable flow zones, since the incidence of flow on a vane extrados takes off and the flow will decrease, so the flow deviates towards the vane. the underside of neighboring dawn which is fed with too strong incidence then takes off and so on, this is related to the speed of rotation.

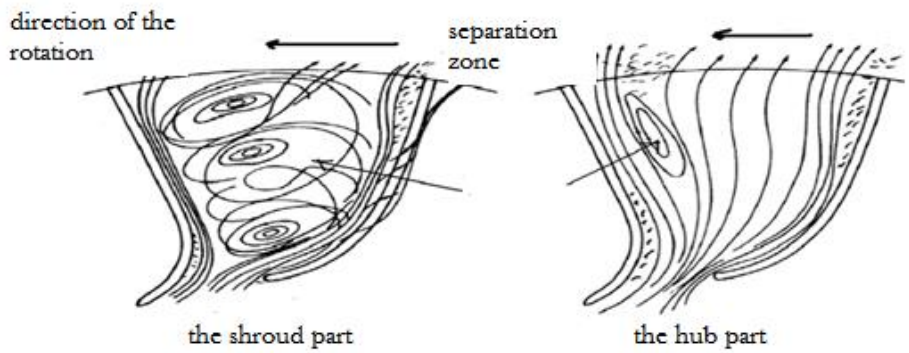

Figure1.10: Presentation of the flow structure in the centrifugal compressor impeller

1.9. The reference planes in centrifugal compressor:

The flows in a centrifugal compressor are three-dimensional, viscous, turbulent and generally compressible fluid . To simplify analysis of the flow cross does in two types of areas of reference fig(1.10)

This decomposition is at the origin of two types of flows : [4]

- Meridian flow.
- The flow dawn to dawn.

For each type of area there are actually an infinite plan 's meridians and dawn-to- dawn, it is generally limited to the study of a single average meridian plane projected on the plane R (z, r) and blade surface to dawn are presented by trans formation compliant in the planR (z, r) e n following the law:

$$d\theta = {}^{dm}/_{r \cdot \tan(\beta)} \qquad (1.27)$$

and the orthogonal cuts which can be considered quasi-planar see figure (1.10)

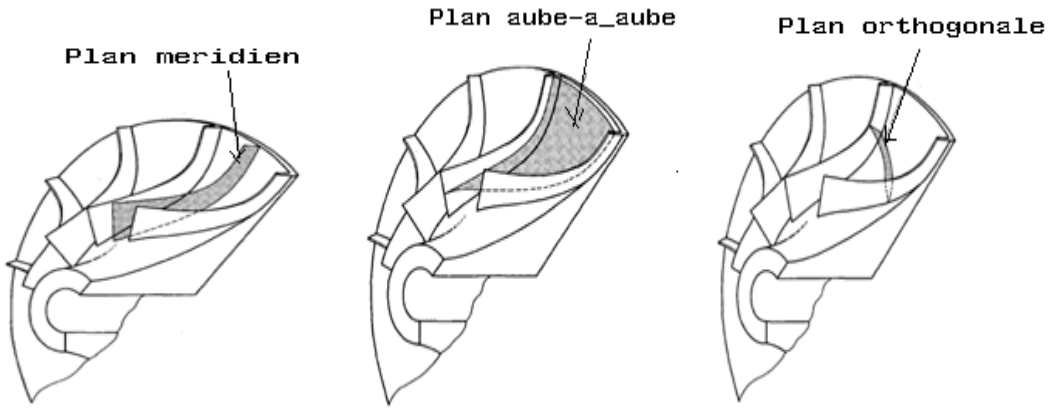

Figure 1.11:the reference surfaces in the centrifugal compressor wheel

1.10. Flow between crankcase and wheel :

The clearance is a very small distance between the end of a blade of the moving wheel and the casing .

The Flows in this area is greatly unstationary and depends on several parameters, such as the shape of the to be the distribution of fillers, the pressure difference between the intrados and the extrados of each blade and the roughness of the walls (surface condition) . in this area there may :

- A vortex is generated by a leakage flow to the casing because of the pressure difference.
- Yhus a layer of verticality generated in the direction of the displacement of the leakage flow which encounters a discontinuity, this discontinuity leads to the formation of a vortex of angular play when there are interactions with the main flow.

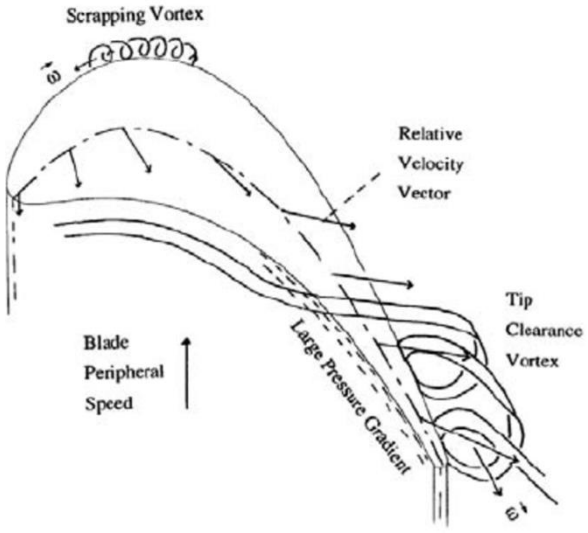

Figure1.12: The effect of wheel-casing clearance in the flow of centrifugal compressors

On the other hand the flow properties in the game have a big impact on the performance of the compressor.

1.11. Jet and wake flow:

The phenomenon of the jet and the wake of the flow occur at the trailing edge of the vanes of the wheel.

The first experimental studies on a centrifugal compressor carried out by D. Eckardt confirmed the Dean and Senoo and Dean theories, which assume the existence of a so-called jet flow structure. and wake at the exit of the moving wheel composed of two zones: A low energy fluid accumulation zone in which the flow is called Wake has been observed, and other high energy zones in which the flow is called Jet.

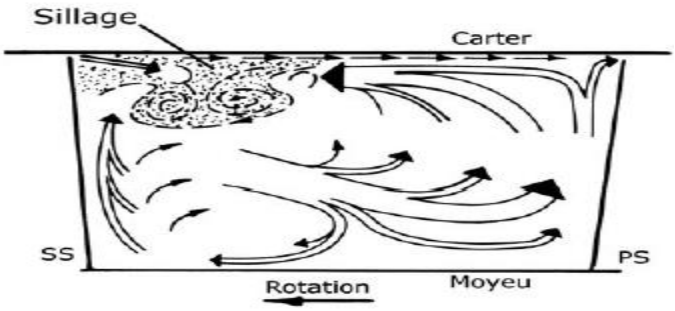

Figure 1.13: Presentation of the Jet and Wake at the exit of the compressor wheel

According to experimental measurements , the structure of the Jet and Silage flow has caused the separation of the boundary layer near the quarter-side of the vanes (the lower surface and the upper surface) where the pressure is lower .

The experimental analysis and the numerical study of the flow structure in a centrifugal compressor carried out by C.Hirsch, S.Kang and G.Pointet and attribute the formation to the exit of the wheel. Jet and wake flow due to the effects of secondary flows.

In 2003 ONERA was doing an analysis on the flow in a centrifugal wheel which explains the phenomenon of Jet and Sillage as being the result of the effects of the secondary flows.

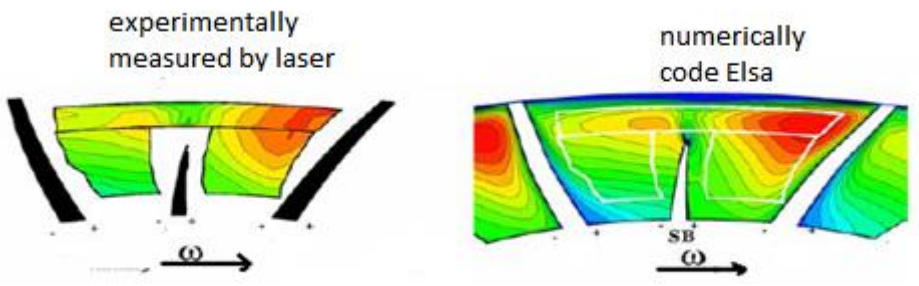

Figure 1.14: Jet and Wake presentation at the exit of the centrifugal compressor wheel [6]

1.12. Secondary flow:

The secondary flow is defined as the components of the relative velocities in the plane orthogonal to the direction of the main flow. [6]

According to Brads how, the swirling flows of secondary flows are formed because of the viscous effects on the crankcase and hub walls that produce a deflection of the main flow.

The characteristics of the secondary flow are:

- a strongly three-dimensional and in-stationary character.
- the presence of longitudinal verticities.
- a strong interaction with the main flow.

CHAPTER 2

2.1. Introduction

In a turbomachine, the flow is generally compressible. The study of this flow, on the impeller of a centrifugal compressor is based on the relations called aerothermodynamics one - dimensional.

Below presentationare different stations of a centrifugal compressor in the meridian plane R (z, r).

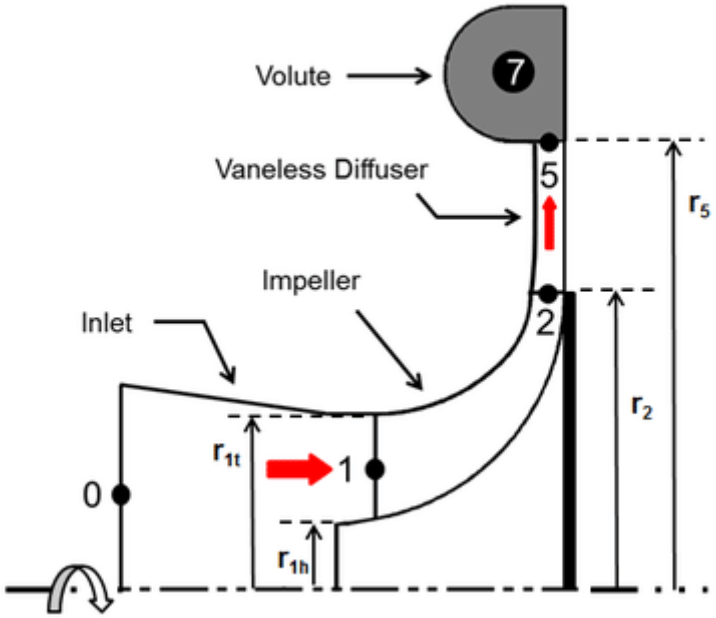

Figure 2.1: the different positions of the sections on a plane R (z, r)

(0) : far section at the wheel entry
(1) : section at the entry of the moving wheel
(2) : outlet section of the moving wheel , and section at the inlet of the radial diffuser. The moving wheel and diffuser section is the smooth diffuser.
(5) :output section of the axial diffuser.

2.2. Mono-dimensional analysis of the flow

2.2.1. Velocity triangle:

The fluid has an absolute speed C_1 at the inlet of the centrifugal compressor wheel, which breaks down as soon as it is driven by the rotation of the latter, into U_1 drive speed,

which is tangent to the internal circumference of the moving wheel, andW_1, relative speed, which is the speed at which the fluid slides on the surface of the blade.

At the exit, the participation envisaged at a driving speedU_2, tangent to the outer circumference of the moving wheel, and a relative speed W_1tangent to the last vane, as soon as the participation leaves the wheel, these two speeds are composed for old absolute speed C_2output.

The velocity equation given by:

$$\vec{C} = \vec{U} + \vec{W} \tag{2.1}$$

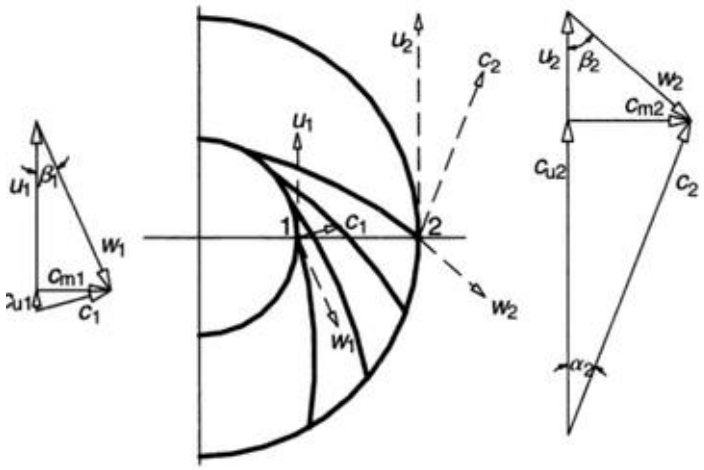

Figure 2.2: Triangle speed at the inlet and outlet of the wheel[1]

2.2.2. The wheel entry:

Represent the triangle of speed:

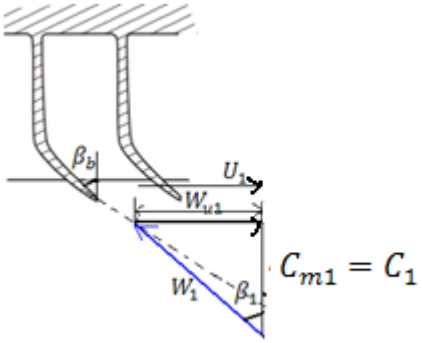

Figure 2.3: Speed triangle at the entrance of the moving wheel

$$C_{m1} = C_1 \tag{2.2}$$

$$\overrightarrow{C_1} = \overrightarrow{W_1} + \overrightarrow{U_1} \tag{2.3}$$

$$\left|\overrightarrow{U_1}\right| = \left|\overrightarrow{W}_{U1}\right| \tag{2.4}$$

$$C_{m1} = C_1 = \frac{\dot{m}}{\rho_1 \cdot A_1} \tag{2.5}$$

The passage section:

$$A_1 = C_D \cdot \left(r_{tip}^2 - r_{hip}^2\right) \tag{2.6}$$

C_D: This is the flow blocking factor.

A from the triangle s speed s, the relative angle flow can be calculated as follows:

The absolute and relative Mach numbers at the input are respectively given by the equation :

$$M_{abs1} = \frac{C_{m1}}{\sqrt{\gamma \cdot r \cdot T_{1s}}} \tag{2. 7}$$

And the equation:

$$M_{rel} = \frac{W_1}{\sqrt{\gamma \cdot r \cdot T_{1s}}} \tag{2. 8}$$

By applying the Theorem Euler to the output of the wheel is found:

$$\Delta h_t = h_{t2} - h_{t1} = (U_2 \cdot C_{u2} - U_1 . C_{u1}) \tag{2.9}$$

At the inlet, the flow being axial and therefore

$$\Longrightarrow C_{u2} = \frac{C_P \cdot (T_{t2} - T_{t1})}{U_2} \tag{2.10}$$

Calculation of the meridian speed C_{m2}at the wheel outlet:

Conservation of the flow:

$$\dot{m}_1 = \dot{m}_2 = \rho_2 \cdot C_{m2} \cdot A_2 \tag{2. 11}$$

A_2 : represents the flow passage section at the outlet of the wheel

$$A_2 = 2 \cdot \pi \cdot R_2 \cdot b \tag{2. 12}$$

So to determine r the meridian speed we have everything we need :

$$C_{m2} = \frac{\dot{m}_2}{\rho_2 \cdot A_2} \tag{2.13}$$

$$\rho_2 = \frac{P_2}{r \cdot T_2} \tag{2.14}$$

With

$$T_2 = T_{t2} - \frac{C_2^2}{2 \cdot C_p} \tag{2.15}$$

From equations (2. 15) (2. 14) and (2. 13) , there is the equation of the second degree :

$$C_{m2}^2 + \left(2 \cdot \frac{C_p \cdot A_2 \cdot P_2}{\dot{m} \cdot r}\right) \cdot C_{m2} + (C_{u2}^2 - 2 \cdot C_P \cdot T_{t2}) = 0 \tag{2. 16}$$

The solution to this equation is the speed C_{m2} with $\boldsymbol{C_{m2} > 0}$

2.2.3. The wheel outlet: [4]

speed triangle to the output:

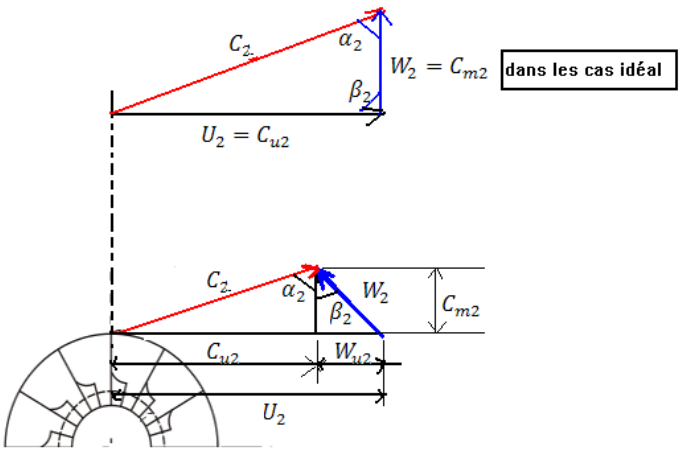

Figure 2.4: Triangle of speed at the output of the moving wheel .

Calculation of angles:

$$\alpha_2 = arct\left(\frac{C_{u2}}{C_{m2}}\right) \tag{2.17}$$

$$\beta_2 = arct\left(\frac{W_{u2}}{C_{m2}}\right) \tag{2. 18}$$

With W_{u2} is the tangential relative speed:

$$W_{u2} = U_2 - C_{u2} \tag{2. 19}$$

The two Mach Numbers are given by:

- Absolute mach :

$$M_{abs2} = \frac{C_{m2}}{\sqrt{\gamma \cdot r \cdot T_2}} \quad (2.20)$$

- Relative Mach :

$$M_{rel2} = \frac{W_2}{\sqrt{\gamma \cdot r \cdot T_1}} \quad (2.\ 21)$$

With :

$$W_2 = \sqrt{C_{m2}^2 + W_{u2}^2} \quad (2.22)$$

The total pressure is given by:

$$P_{t2} = P_2 \cdot \left(\frac{T_{t2}}{T_2}\right)^{\gamma/\gamma-1} \quad (2.23)$$

The isentropic efficiency of the Centrifugal Compressor is calculated by:

$$\eta_{is,Rotor} = \frac{\left(\frac{P_{t2}}{P_1}\right)^{\gamma-1/\gamma} - 1}{\left(\frac{T_{t2}}{T_1}\right)^{\gamma} - 1} \quad (2.\ 24)$$

2.3.Finite difference method:

In numerical analysis, the finite difference method is a common technique for finding approximate solutions of partial differential equations which consists in solving a system of relations (numerical scheme) linking the values of the unknown functions at certain points sufficiently close to each other.

This method appears to be the simplest to implement because it proceeds in two stages: on the one hand the discretization by finite differences of the operators of derivation / differentiation, on the other hand the convergence of the numerical diagram thus obtained when the distance between the points decreases. [7]

For the finite difference method, a mesh is a set of isolated points (called nodes) located in the domain of definition of the functions subjected to partial differential equations, a grid on the only nodes of which are defined the unknowns corresponding to the approximate values of these functions .

The mesh also includes nodes located on the border of the domain (or at least "close" to this border) in order to be able to impose the boundary conditions and / or the initial condition with sufficient precision.

A priori, the first quality of a mesh is to cover as well as possible the domain in which it develops, to limit the distance between each node and its nearest neighbor. However, the mesh must also make it possible to express the discrete formulation of the differentiation operators: for this reason, the nodes of the mesh are most often located on a grid whose main directions are the axes of the variables.

The distance between two neighboring nodes located on a straight line parallel to one of the axes is not called a mesh. In this sense, the step is a notion both local and directional. We will speak of global step to designate the largest local step, a notion which remains directional.

Although a constant step is most often retained (without it posing a theoretical problem for the resolution), it is sometimes judicious to introduce a variable step which will be chosen finer in the zones where the exact solution undergoes more large variations: this tip helps reduce the number of unknowns without compromising the accuracy of the results. On the other hand, the formulation is a little more complex because the discretization of the differential operators must take it into account

2.4.Finite Volume Method:

2.4.1.introduction:

The finite-volume method discretizes the integral form of the conservation equations directly in the physical space. It was initially introduced by researchers such as McDonald (1971) and McCormack and Paullay (1972) for the solution of two-dimensional time-dependent Euler equations and was later extended to three-dimensional flows by Rizzi and Inouye (1973). The computational domain is subdivided into a finite number of contiguous control volumes, where the resulting statements express the exact conservation of relevant properties for each of the control volumes. At the centroid of each of the control volumes, the variable values are calculated. Interpolation is used to express variable values at the control volume surface in terms of the center values, and suitable quadrature formulae are applied to approximate the surface and volume integrals. An algebraic equation for each of the control volumes can be obtained, in which a number of the neighboring nodal values appear.

As the finite-volume method works with control volumes and not the grid intersection points, it has the capacity to accommodate any type of grid. Here, instead of structured grids, unstructured grids can be employed that allow a large number of options for the definition of the shape and location of the control volumes. Since the grid defines only the control volume boundaries, the method is conservative so long as the surface integrals that are applied at these boundaries are the same as the control volumes sharing the boundary. One disadvantage of this method compared with the finite-difference schemes is that higher-order differencing approximations greater than the second order are more difficult to develop in three dimensions. This is because of the requirement for two levels of approximation, which are interpolation and integration. However, the finite-volume method has more advantages than disadvantages. One important feature of the method is that a 'finite-element'-type mesh can be used, which the mesh can be formed by the combination of triangles or quadrilaterals in the case of two dimensions or tetrahedral and hexahedra in three dimensions. This type of unstructured mesh offers greater flexibility for handling complex geometries. Another attractive feature is the method requires no transformation of the equations in terms of body-fitted coordinate system as is required in finite-difference method.

Compared to the classical finite difference method (FDM) the FVM has the following advantages:

1. Spatial discretisation is totally flexible: the mesh can accommodate to irregularly shaped boundaries toreduce geometric errors and the mesh can be refined locally to give more resolution in regions of particularinterest.

2. Equations are presented in *integral form* which is often how they are derived from the underlying physicallaws.

3. Because of (2) there is no need for dependent variables to be differentiable everywhere which means that alarger class of problems can be solved.

4. The FVM naturally conserves conserved variables when applied to PDEs expressing conservation laws since,as two neighboring cells share a common interface, the total flow of a conserved quantity out of one cell willbe the same as that entering the other cell.

One disadvantage of the FVM over the FDM is that there is no easily accessible underlying theory (e.g. for formalaccuracy). However a FVM on a uniform Cartesian mesh can be regarded as a FDM which then permits analysis basedon Taylor series. [8]

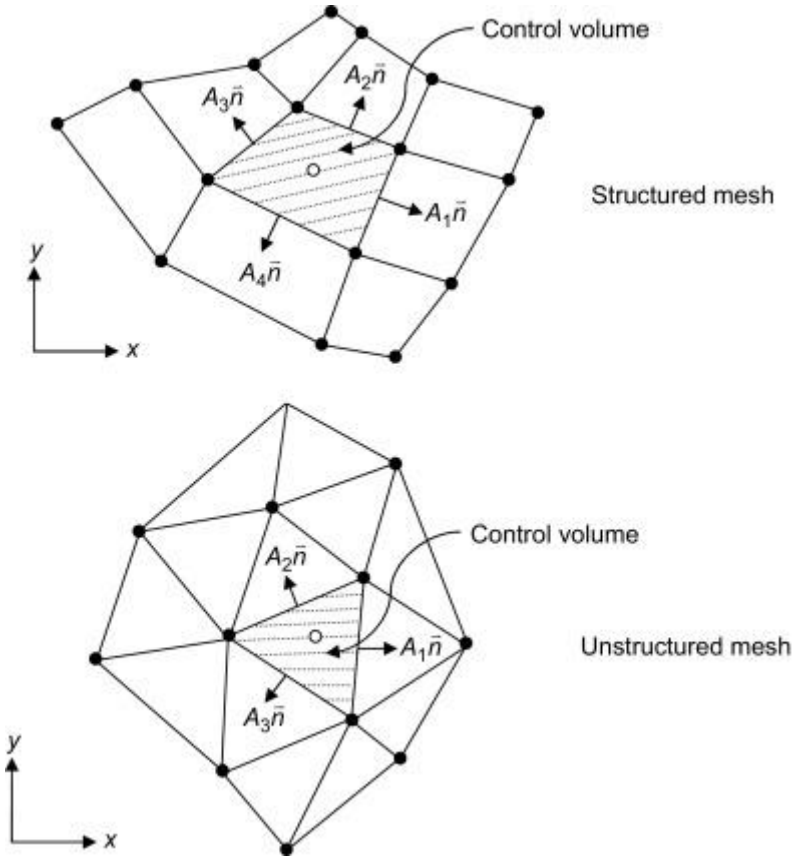

Figure2.5: A representation of structured and unstructured mesh for the finite-volume method (full symbols denote element vertices, and open symbols at the centre of the control volumes denote computational nodes).

2.4.2 Basic equations:

The FVM can be used in 1D, 2D or 3D but a 2D treatment best encapsulates its essential elements and may be generalized easily to other dimensions and also to systems of equations. Consequently we will develop the FVM formulation for a 2D geometry[9]

- **The continuity equation:**

$$\frac{\partial \rho}{\partial t} + \frac{\partial \left(\rho \cdot U_j \right)}{\partial x_j} = 0 \tag{2.25}$$

- **The momentum equation:**

$$\frac{\partial (\rho \cdot U_i)}{\partial t} + \frac{\partial \left(\rho \cdot U_j \cdot U_i \right)}{\partial x_j} = -\frac{\partial p}{\partial x_i} + \frac{\partial}{\partial x_j} (\mu_{eff} \cdot (\frac{\partial U_i}{\partial x_j} + \frac{\partial U_j}{\partial x_i})) + S_u \tag{2. 26}$$

- **The overall equation:**

$$\underbrace{\frac{\partial(\rho\cdot\phi_i)}{\partial t}}_{1}+\underbrace{\frac{\partial\left(\rho\cdot U_j\cdot\phi_i\right)}{\partial x_j}}_{2}=\underbrace{\frac{\partial}{\partial x_j}(\Gamma_{eff}\cdot(\frac{\partial\phi_i}{\partial x_j})}_{3}+S_{\phi}{}_{4} \qquad (2.27)$$

Or :
1: the transient term.
2: the convective term.
3: the diffusive term.
4: the source term.
∅: Any scalar quantity (variable).
$_{eff}$: Diffusion coefficient of the quantity ∅ to be transported.

These equations are integrated on each control volume, to convert certainvolume integrals to surface integrals, we used the divergence theorem ofGauss such as

$$\int_V\frac{\partial B_j}{\partial x_j}dV=\int_A B_j\cdot n_j\cdot dA \qquad (2.28)$$

B_j: It's any vector.

n_j: It is a unit vector at the surface A surrounding the control volumeV

If the control volume does not deform over time, the derivatives with respect to thetime can be placed outside the integral of the volume and the equations becomeso:

- **The continuity equation:**

$$\frac{d}{dt}\int_V\rho\cdot dv+\int_A\rho\cdot U_j\cdot n_j\cdot dA=0 \qquad (2.29)$$

- **The momentum equation:**

$$\frac{d}{dt}\int_V\rho\cdot U_i\cdot dv+\int_A\rho\cdot U_j\cdot U_i\cdot n_j\cdot dA=-\int_A p\cdot n_j\cdot dA+\int_A\mu_{eff}\cdot(\frac{\partial U_j}{\partial x_i}+\frac{\partial U_i}{\partial x_j})\cdot n_j\cdot dA+\int_V S_{ui}\cdot dv \qquad (2.30)$$

- **The overall equation:**

$$\frac{d}{dt}\int_V\rho\cdot\phi\cdot dv+\int_A\rho\cdot U_j\cdot\phi\cdot n_j\cdot dA=\int_A\Gamma_{eff}\cdot(\frac{\partial\phi}{\partial x_j})\cdot n_j\cdot dA+\int_V S_\phi\cdot dv \qquad (2.31)$$

Where V and A are respectively, control volume and regions of the integration surface,and j n are the components of the normal vector at the surface always directed outwards(out of volume).

The volume integrals represent the source or accumulation terms and theSurface integrals represent the sum of the flows.The first step in the numerical solution of these exact differential equations isto create a compiled system of linearization of algebraic equations. This is done byconverting each term into a discrete form.Consider for example an element of an isolated mesh as below;

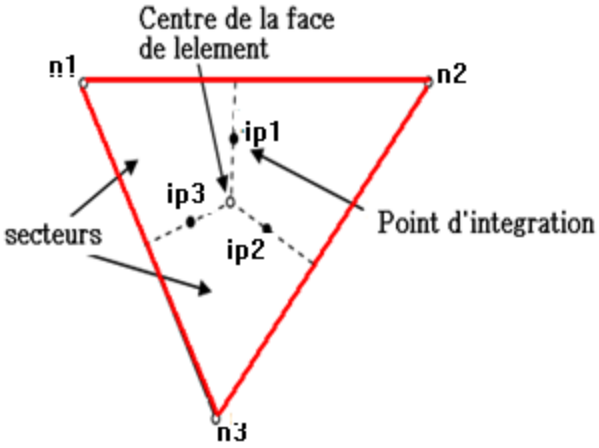

Figure2.6: Integration point in an element of a control volume.

Either the source or the accumulation, they are converted in terms of discrete formsin each sector composing the specific control volume, then integrated on allthe areas of the control volume.

As for the term of the surface flux, it is converted into a discrete form at the pointip integration, which are located at the center of each surface segment in an elementthree-dimensional, then distributed to the adjacent control volume. Surface flows inan integration point of two adjacent volumes are equal and opposite, the surface floware therefore locally conserved quantities, then evaluated by integrating the flows onthe surface segments that contribute to a control volume.There are several discrete approximations developed in CFDs, which are based onapproximations of series development of continuous functions (such as the series ofTaylor).

The order and precision of the approximation are determined by the exponent of the spacingof stitches where the most important factor is the time step, the increase in order andthe precision of an approximation generally implies that the errors are reduced morequickly, but this increases the computational load, plus the order approximationshigh are generally less stable numerically

2.5Nature Of Turbulence

2.5.1 Introduction:

Turbulence is a kind of fluid motion which is:

- UNSTEADY and highly IRREGULAR in space and time
- 3-DIMENSIONAL
- always ROTATIONAL and at HIGH REYNOLDS NUMBERS
- DISSIPATIVE
- strongly DIFFUSIVE

Turbulent fluctuations can generate rates of momentum transfer far greater than those due to molecular diffusion.

The turbulent motion has a wide spectrum of eddy sizes, and large and small eddies can coexist in the same volume of fluid.

The LARGEST eddies are associated with LOW frequency fluctuations, as large as the dimensions of the flow, and responsible for most of the momentum transport. The SMALLEST eddies are associated with HIGH frequency fluctuations, and are determined by viscous forces.

2.5.2. Simulation of Turbulent Flows:

Currently, three approaches are available. Each approach offers a degreeof different resolution. [11]

- **Direct Numerical Simulation**

(DNS): allows the resolution of all spatial scales andtemporal. This approach provides full resolution withoutno modeling. However, this approach is too expensive forindustrial flows.

- **Large Eddy Simulation (LES):**

Consists in solving the spatial and temporal scales which cover thehigh energy structures. The large vortices aredirectly resolved; the little ones are modeled. This approach is lessexpensive than the DNS, but very often still too expensive for theindustrial applications.

- **The Reynolds-averaged Navier-Stokes (RANS) approach:**

consists of solving only the middle part of the flow andmodel the turbulence scales. The solution is given bytime-averaged equations. This is the most widely used approachused for industrial flows.A simulation of the RANS equations considerably reduces the effortsof calculation compared toa direct digital simulation (DNS) or a simulation of large scales(LES) and it is widely used for engineering calculations. Forsave computing resources, the averaged approach (RANS) is usedfor this research project. The turbulence models available in ANSYS CFX

2.5.3.presentation of turbulence model:

- **k-ε standard:**

The K-epsilon model is one of the most common turbulence models, although it just doesn't perform well in cases of large adverse pressure gradients It is a two equation model that means, it includes two extra transport equations to represent the turbulent properties of the flow. This allows a two equation model to account for history effects like convection and diffusion of turbulent energy. [10]

The first transported variable is turbulent kinetic energy, k. The second transported variable in this case is the turbulent dissipation, ε. It is the variable that determines the scale of the turbulence, whereas the first variable, k, determines the energy in the turbulence.

There are two major formulations of K-epsilon models (see References[12] for more information). That of Launder and Sharma is typically called the "Standard" K-epsilon Model. The original impetus for the K-epsilon model was to improve the mixing-length model, as well as to find an alternative to algebraically prescribing turbulent length scales in moderate to high complexity flows.

As described in Reference[13] "Turbulence Modeling Validation, Testing, and Development", NASA Technical Memorandum 110446.), the K-epsilon model has been shown to be useful for free-shear layer flows with relatively small pressure gradients. Similarly, for wall-bounded and internal flows, the model gives good results only in cases where mean pressure gradients are small; accuracy has been shown experimentally to be reduced for flows containing large adverse pressure gradients. One might infer then, that the K-epsilon model would be an inappropriate choice for problems such as inlets and compressors.

Transport equations for standard k-epsilon model

- For turbulent kinetic energy k:

$$\frac{\partial(\bar{\rho}\cdot k)}{\partial t}+\frac{\partial}{\partial x_j}\left(\bar{\rho}\cdot\widetilde{u_j}\cdot k\right)=\frac{\partial}{\partial x_j}\left[\left(\mu+\frac{\mu_T}{\sigma_k}\right)\frac{\partial k}{\partial x_j}\right]+P_k-\bar{\rho}\cdot\varepsilon \tag{2.32}$$

- For dissipation ε :

$$\frac{\partial(\bar{\rho}\cdot\varepsilon)}{\partial t}+\frac{\partial}{\partial x_j}\left(\bar{\rho}\cdot\widetilde{u_j}\cdot\varepsilon\right)=\frac{\partial}{\partial x_j}\left[\left(\mu+\frac{\mu_T}{\sigma_\varepsilon}\right)\frac{\partial\varepsilon}{\partial x_j}\right]+\frac{\varepsilon}{k}\left(C_{\varepsilon1}\cdot P_k-C_{\varepsilon2}\cdot\bar{\rho}\cdot\varepsilon\right) \tag{2.33}$$

- Modeling turbulent viscosity:

$$\mu_t=\rho C_\mu\frac{K^2}{\epsilon} \tag{2.34}$$

- Production of k:

$$P_k=-\overline{\rho u_i' u_j'}\frac{\partial u_j}{\partial x_i} \tag{2.35}$$

$$P_k=\mu_t S^2$$

Where Sis the modulus of the mean rate-of-strain tensor, defined as:

$$S=\sqrt{2S_{ij}S_{ij}} \tag{2.36}$$

Effect of buoyancy

$$P_b=\beta g_i\frac{\mu_t}{Pr_t}\frac{\partial T}{\partial x_i} \tag{2.37}$$

Where $\mathbf{P_{rt}}$ is the turbulent Prandtl number for energy and gi is the component of the gravitational vector in the ith direction. For the standard and realizable - models, the default value of Prt is 0.85.

The coefficient of thermal expansion,β , is defined as:

$$\beta = -\frac{1}{\rho}\left(\frac{\partial \rho}{\partial T}\right) \tag{2.38}$$

Model constants:

C_μ	C_{z1}	C_{z2}	σ_k	σ_z
0.09	1.44	1.92	1.0	1.3

- **RNG k-epsilon model**

The RNG model was developed using Re-Normalisation Group (RNG) methods by Yakhot et al to renormalize the Navier-Stokes equations, to account for the effects of smaller scales of motion. In the standard k-epsilon model the eddy viscosity is determined from a single turbulence length scale, so the calculated turbulent diffusion is that which occurs only at the specified scale, whereas in reality all scales of motion will contribute to the turbulent diffusion. The RNG approach, which is a mathematical technique that can be used to derive a turbulence model similar to the k-epsilon, results in a modified form of the epsilon equation which attempts to account for the different scales of motion through changes to the production term.

Transport Equations

There are a number of ways to write the transport equations for k and ε, a simple interpretation where bouyancy is neglected is:

$$\frac{\partial(\rho \cdot k)}{\partial t} + \frac{\partial}{\partial x_i}(\rho k u_i) = \frac{\partial}{\partial x_j}\left[(\mu + \frac{\mu_T}{\sigma_k})\frac{\partial k}{\partial x_j}\right] + P_k - \rho \cdot \varepsilon \tag{2.39}$$

$$\frac{\partial(\rho \varepsilon)}{\partial t} + \frac{\partial}{\partial x_i}(\rho \varepsilon u_i) = \frac{\partial}{\partial x_j}\left[(\mu + \frac{\mu_T}{\sigma_\varepsilon})\frac{\partial \varepsilon}{\partial x_j}\right] + C_{1\varepsilon}\frac{\varepsilon}{k}P_k - C_{2\varepsilon}^{*}\frac{\varepsilon^2}{k} \tag{2.40}$$

Where :

C_μ	$C_{\varepsilon 1}$	$C_{\varepsilon 2}$	σ_k	σ_ε	β
0.0845	1.42	1.68	0.7194	1.3	0.012

Applicability and use:

Although the technique for deriving the RNG equations was quite revolutionary at the time, it's use has been more low key. Some workers claim it offers improved accuracy in rotating flows, although there are mixed results in this regard: It has shown improved results for modelling rotating cavities, but shown no improvements over the standard model for predicting vortex evolution.

- **K omega model:**

This turbulence model uses two transport equations, an equation ofdissipation transport ε and the other equation proposed by Wilcox using the turbulence frequency ω. The two variables are linked by the following formula:

$$\varepsilon = \beta^* \cdot \omega \cdot k \tag{2.41}$$

The stress tensor is calculated from Foucault:

$$\mu_t = \rho \cdot \frac{k}{\omega} \tag{2.42}$$

The turbulent kinetic energy equation:

$$\frac{\partial(\bar{\rho}\cdot k)}{\partial t} + \frac{\partial}{\partial x_j}\left(\bar{\rho}\cdot\widetilde{u_j}\cdot k\right) = \frac{\partial}{\partial x_j}\left[(\mu + \frac{\mu_T}{\sigma_{k1}})\cdot\frac{\partial k}{\partial x_j}\right] + P_k - \beta\cdot\bar{\rho}\cdot k\cdot\omega \tag{2.43}$$

- **k − ω SST:**

Combination of the model k − ω near the walls and of k − ϵ at the heart of the flow.Model with 2 transport equations.More interesting to test than the k – ω standard.

It is widely accepted that the Navier-Stokes (NS) equations together with the continuity equation comprise a closed set of equations, the solution of which provides a valid description of laminar and turbulent flows.

For an incompressible flow, these equations are:

$$\frac{\partial U_i}{\partial x_i} = 0 \tag{2.44}$$

$$\rho \frac{\partial U_i}{\partial t} + \rho \sum_j \frac{\partial (U_i U_j)}{\partial x_j} = -\frac{\partial P}{\partial x_i} + B_i + \rho \sum_j \frac{\partial}{\partial x_j}\left[\vartheta_L \left(\frac{\partial U_i}{\partial x_j} + \frac{\partial U_j}{\partial x_i}\right)\right] \tag{2.45}$$

The equations for a scalar quantity C, such as species concentration, and an energy variable, such as enthalpy h, are:

$$\rho \frac{\partial C}{\partial t} + \rho \sum_j \frac{\partial (U_j C)}{\partial x_j} = \rho \sum_j \frac{\partial}{\partial x_j}\left[\frac{\vartheta_L}{Pr_L(C)} \frac{\partial C}{\partial x_j}\right] \tag{2.46}$$

$$\rho \frac{\partial h}{\partial t} + \rho \sum_j \frac{\partial (U_j h)}{\partial x_j} = \rho \sum \frac{\partial}{\partial x_j}\left[\frac{\vartheta_L}{Pr_L(h)} \frac{\partial h}{\partial x_j}\right] + S \tag{2.48}$$

It is possible, in principle, to simulate any turbulent flow by solving the foregoing exact equations with appropriate boundary conditions using suitable numerical procedures such as embodied in PHOENICS.

Such a calculation is called DIRECT NUMERICAL SIMULATION, but in practice it is rarely done.

This is because of the need to represent all eddies from the smallest scale, corresponding to the dissipative motions, to the largest scale, corresponding to the largest dimension. Further, the time step chosen for the simulations must be sufficiently small to resolve the fastest fluctuations.

For the values of Reynolds numbers encountered in practical engineering flows, the computational effort is prohibitive.

There are essentially two alternative routes for the prediction of turbulent flows:

- LARGE-EDDY SIMULATION (LES) and
- TURBULENCE MODELLING.

LES involves:

- the solution of the 3D time-dependent NS equations
- direct simulation of the large-scale motion; and
- use of a sub-grid-scale (SGS) model for turbulence of scales smaller than the computational grid spacing.

The advantages of LES arise from the fact that the large eddies, which are hard to model in a universal way, are simulated directly.

The application of LES to practical flows has been limited because of:

- prohibitive expense at high Reynolds number;
- the difficulties in specifying initial and boundary conditions; and the need to perform 3D time-dependent simulations, even if the flow is 2D and statistically stationary!

2.5.4.Turbulence Modelling

Engineers are not concerned with all the details of the turbulent motion, but rather with its effects on the gross properties of the flow. Consequently, there is no need to solve for the INSTANTANEOUS variables if AVERAGED variables are all that is required. [14]

The instantaneous variables are decomposed into MEAN and FLUCTUATING quantities:

$$U_i = \bar{U}_i + u_i \ , P = \bar{P} + p \ , H = \bar{H} + h \ , C = \bar{C} + c$$

Where the mean values are obtained by averaging over a time scale, dt, which is long compared to that of turbulent motion, and in unsteady problems small compared with the unsteadiness of the mean motion.

The definitions of instantaneous quantities are substituted into the equations of the instantaneous motion, which are then averaged to produce the equations of the mean motion.

For an incompressible flow, the AVERAGED equations are:

$$\frac{\partial U_i}{\partial x_i} = 0 \qquad (2.49)$$

$$\rho \frac{\partial U_i}{\partial x_i} + \rho \sum_j \frac{\partial (U_i U_j)}{\partial x_j} = -\frac{\partial P}{\partial x_i} + B_i + \rho \sum_j \frac{\partial}{\partial x_j}\left[\vartheta_L \left(\frac{\partial U_i}{\partial x_j} + \frac{\partial U_j}{\partial x_i}\right) - \overline{u_i u_j}\right] \quad (2.50)$$

$$\rho \frac{\partial C}{\partial t} + \rho \sum_j \frac{\partial (U_j C)}{\partial x_j} = \rho \sum_j \frac{\partial}{\partial x_j}\left[\frac{\vartheta_L}{Pr_L(C)} \frac{\partial C}{\partial x_j} - \overline{u_i c}\right] \quad (2.51)$$

$$\rho \frac{\partial H}{\partial t} + \rho \sum_j \frac{\partial (U_j H)}{\partial x_j} = \rho \left[\frac{\vartheta_L}{Pr_L(H)} \frac{\partial H}{\partial x_j} - \overline{u_i h}\right] + S \quad (2.52)$$

The statistical-averaging process has introduced unknown turbulent correlations into the mean-flow equations which represent the turbulent transport of momentum, heat and mass - the REYNOLDS STRESSES and FLUXES. In general, there are:

- 6 Reynolds stress components: $-u_i u_j$
- 3 Reynolds enthalpy flux components: $-u_i h$
- 3 Reynolds mass flux components: $-u_i c$

A TURBULENCE MODEL can be described as a set of relations and equations needed to determine the unknown turbulent correlations that have arisen from the averaging process.

Turbulence models of various complexity have been developed, and with very few exceptions, they can be classified as EDDY-VISCOSITY MODELS or REYNOLDS-STRESS MODELS.

In EDDY-VISCOSITY MODELS, the unknown correlations are assumed to be proportional to the spatial gradients of the quantity they are meant to transport.

In REYNOLDS-STRESS MODELS, the unknown correlations are determined directly from the solution of differential transport equations in which they are the dependent variables.

- **Eddy-Viscosity Concept**

Most turbulence models use the eddy-viscosity concept to determine the Reynolds stresses from:

$$-\rho \overline{u_i u_j} = \mu_t \left(\frac{\partial U_i}{\partial x_j} + \frac{\partial U_j}{\partial x_i}\right) - \rho \times KE \frac{2 d_{ij}}{3} \quad (2.53)$$

Where$\mu_{\mu t}$is the eddy viscosity and KE is the turbulent kinetic energy.

$\mu_{\mu t}$isnot a fluid property; it depends on the state of turbulence and must be determined by the turbulence model.

For enthalpy and mass transfer, the Reynolds fluxes are determined from:

$$-\rho\overline{u_i h} = \frac{\mu_t}{Pr_t(H)}\frac{\partial H}{\partial x_i}, -\rho\overline{u_i c} = \frac{\mu_t}{Pr_t(C)}\frac{\partial C}{\partial x_i} \quad (2.54)$$

Where $Pr_t(H)$ and $Pr_t(C)$ are turbulent Prandtl and Schmidt numbers, which are approximately unity.

For dimensional reasons,$\mu_t$is proportional to:$\mu_t = C\rho V_s L_s$

Where C is an empirical constant, and V_s and L_s are turbulence velocity and length scales which characterize the LARGE-SCALE turbulent motion.

The simplest turbulence model is one which uses a constant value for the eddy viscosity. It is often convenient to use this very simple model whilst the main features of the CFD simulation are being put together. A more accurate turbulence model can be introduced at a later stage.

A reasonable value of the kinematic eddy viscosity $ENUT = \frac{\mu_t}{\rho}$ can be estimated by taking: C=0.01; V_s as a typical mean-flow velocity, say the bulk value; and the length scale L_s as ~10% of the flow width.

2.5.5. Classification Of Turbulence Models :

- **ZERO-EQUATION MODELS:** V_s and L_s are calculated directly from the local mean flow quantities (e.g. Prandtl's mixing-length model).
- **ONE-EQUATION MODELS**: V_s is calculated from a suitable transport equation, usually the turbulent kinetic energy, KE, and the length scale, L_s, is prescribed empirically (e.g. Prandtl's k-L model).
- **TWO-EQUATION MODELS:** V_s and L_s are both calculated from transport equations, usually KE and its dissipation rate EP.

- **REYNOLDS-STRESS/FLUX TRANSPORT MODELS:** These are models involving the solution of transport equations for the Reynolds stresses and fluxes, together with a transport equation for the length scale, usually EP.
- **ALGEBRAIC STRESS/FLUX MODELS:** These models simplify the stress/flux transport equations to provide algebraic expressions for the turbulent correlations, which are then solved together with a 2-equation model.[1]

Where:

V_s is a typical velocity scale, L_s a typical length scale, and C is a constant the order of 0.01.

2.6. Reynolds-Stress Transport Model

In general the Reynolds-stress transport model (RSTM) involves the solution of the following turbulence transport equations:[15]

- 3 normal stresses
- 3 shearing stresses
- The dissipation rate EP
- 3 enthalpy fluxes, and 3 mass fluxes per scalar variable

The 3 normal stresses are always solved, but the shearing stresses are solved only when the appropriate velocity components are solved.

The Reynolds-stress transport equations may be written in the following symbolic tensor form:

$$T_{ij} + C_{ij} = D_{ij} + P_{ij} + R_{ij} - E_{ij} \tag{2.55}$$

Where T_{ij}=transience, C_{ij}=convection, D_{ij}=diffusion, P_{ij}=production, R_{ij}=redistribution and E_{ij}dissipation.

The R_{ij} term is the most important term requiring closure in the RSTM. It is commonly known as the pressure-strain term, and PHOENICS provides for 3 different closure models (IRSMHM,QIM,IPY)which are selected by IRSMHM

The IPM and QIM models are the most commonly used in the literature, while the IPY model performs similarly but offers advantages for swirl flows.

These pressure-strain models require wall-correction terms which are provided by PHOENICS as default through the TURMOD command. The corrections account for wall effects on the redistribution process.

The RSTM itself is activated from the Q1 file by the PIL command

TURMOD(REYSTRS,DTFS,WALL1,WALL2,...)

The wall patches WALL1, WALL2, etc. must be previously defined through laminar wall PATCH and COVAL settings for the velocity variables.

The TURMOD command will then:

1. create COVAL settings for the velocities and EP using GRND2 wall functions
2. create PATCH and COVAL settings for the stress-equation variables so as to represent the wall-damping sources associated with the chosen pressure-strain model
3. create RELAX commands for all Solved variables with a false time step of DTFS

The TURMOD command also activates solution of: the dissipation rate EP; the normal stresses U2RS, V2RS, W2RS; and, as appropriate, the shearing stresses UVRS, UWRS and VWRS.

When heat and/or mass transfer is activated the default is that the turbulent fluxes of energy and scalars are represented by a simple gradient-diffusion model through the default setting IRSMSM=0, i.e.

$$-\rho\overline{u_i h} = \frac{\mu_t}{PRT(h)}\frac{\partial h}{\partial x_i} \quad , \quad -\rho\overline{u_i c} = \frac{\mu_t}{PRT(c)}\frac{\partial c}{\partial x_i} \tag{2.56}$$

Where $$\mu_t = \frac{\rho C_\mu C_d KE^2}{EP} \tag{2.57}$$

And $$C_\mu C_d = 0.255 \tag{2.58}$$

The generalized gradient-diffusion model can be activated by setting IRSMSM=1, in which case the Reynolds fluxes are computed from:

$$-\rho\overline{u_i h} = C_t\overline{u_i u_j}\frac{KE}{EP}\frac{\partial h}{\partial x_i} \tag{2.59}$$

Where the coefficient C_t=0.3. The command IRSMSM must appear before the TURMOD command in the Q1 file.

The full Reynolds-flux transport model can be activated by setting IRSMSM=2 before the TURMOD command in the Q1 file. The flux transport equations may be written in the following symbolic tensor form:$T_i + C_i = D_i + P_i + R_i$

Where T_i=transience, C_i=convection, D_i=diffusion, P_i=production, and R_i=pressure-scrambling. The R_i term requires wall-correction terms which are provided by PHOENICS as default through the TURMOD command.

If H1 or TEM1 are stored, TURMOD automatically sets:

- STORE(UTRS) if NX > 1
- STORE(VTRS) if NY > 1
- STORE (WTRS) if NZ > 1 and .NOT. PARAB

Likewise, if SC1, SC2, SCn, etc., are STOREd, storage is provided as appropriate for USC1, USC2, USCn, VSC1, VSC2, VSCn, WSC1, WSC2, WSCn etc.

If IRSMSM=2 the procedure is the same excepting that SOLVE replaces STORE because transport equations will now be solved for each of the individual flux components.

In addition, wall damping sources are created for these components, and if U1 is SOLVEd and NX=1 then UTRS, USC1, USC2, USCn are also SOLVEd.

The advantage of the RSTM is that it provides a more rigorous and realistic approach, and it captures anisotropic effects automatically.

However, RSTMs are much more complex than eddy-viscosity models, and they are computationally more expensive and less stable.

2.7.Near-Wall Approaches

The wall no-slip condition ensures that over some region of the wall layer, viscous effects on the transport processes must be large.

The representation of these processes within a CFD model raises 2 problems:

1. How to account for viscous effects at the wall.

2. How to resolve the rapid variation of flow variables which occurs within this region, without using a very fine computational mesh.

There are two methods:

- the WALL-FUNCTION method and
- the LOW-REYNOLDS-NUMBER method

For the Wall-Function Method, the viscous sublayer is bridged by employing empirical formulae to provide near-wall boundary conditions for the mean flow and turbulence transport equations.

These formulae connect the wall conditions (e.g. the wall shear stress) to the dependent variables at the near-wall grid node which is presumed to lie in fully-turbulent fluid.

Strictly, wall functions should be applied to a point whose Y^+ value is in the range $30 < Y^+ < 130$, where:

$$Y^+ = \frac{U_S Y}{ENUL} \tag{2.60}$$

AndU_S is the friction velocity. The user may elicit printout of Y^+ in the RESULT file by setting YPLS=T or WALPRN=T in the Q1 file. If in addition, STORE(YPLS) appears UP> is written to both the PHI and RESULT files.

The advantages of this approach are that it escapes the need to extend the computations right to the wall, and it avoids the need to account for viscous effects in the turbulence model.[16]

CHAPTER 3

Software Presentation and Numerical Modeling

3.1.Introduction

Today, thanks to the development of digital simulation tools and the power of computer resources, there are a large number of computer codes dedicated to the treatment of complex three-dimensional problems, particularly in the fields of fluid mechanics and turbomachines. The most famous calculation codes are: ANSYS CFX, GAMBIT, FLUENT, STAR-CD, FEMLAB, NUMECA … etc.

The software used in this work, to digitally model the compressible flow in a centrifugal compressor, is ANSYS-CFX 12.1.

3.2.Presentation of the CFX -11software:

CFX is a generic name of the ATA-Technology company which brings together a set of digital CFD (Computational Fluid Dynamics) tools. This software offers many multiphase models and digital diagrams with which the user is normally able to model a wide range of fluid mechanics problems.

Like many software, the CFX-11 includes several tools and modules for:

- drawing (creation of geometries).
- mesh generation (stucco or non-stucco)
- the calculation.

The study of the different parts of the turbomachine using the CFX 12.1 software is done step by step, in each step the software uses some of its tools or components,

- **ANSYS BladeGen**: Generation of the centrifugal compressor wheel
- **ANSYS TurboGrid**: Generation of the structured mesh
- **ANSYS CFX-pre-processor**: Boundary conditions
- **ANSYS CFX-solver**: Resolution of equations of motion and transport
- **ANSYS CFX-poste-traitement**: Presentation of results

3.2.1.ANASYS CFX –Blade Gen V-11:

The first step of resolution consists in defining the geometry of the impeller of the Centrifugal Compressor by CFX –Blade Gen. It is a three-dimensional tool, quick to use to create geometry, specialized in the field of Turbomachines, namely: Compressors (centrifugal or axial), pumps, fans, turbines….etc.

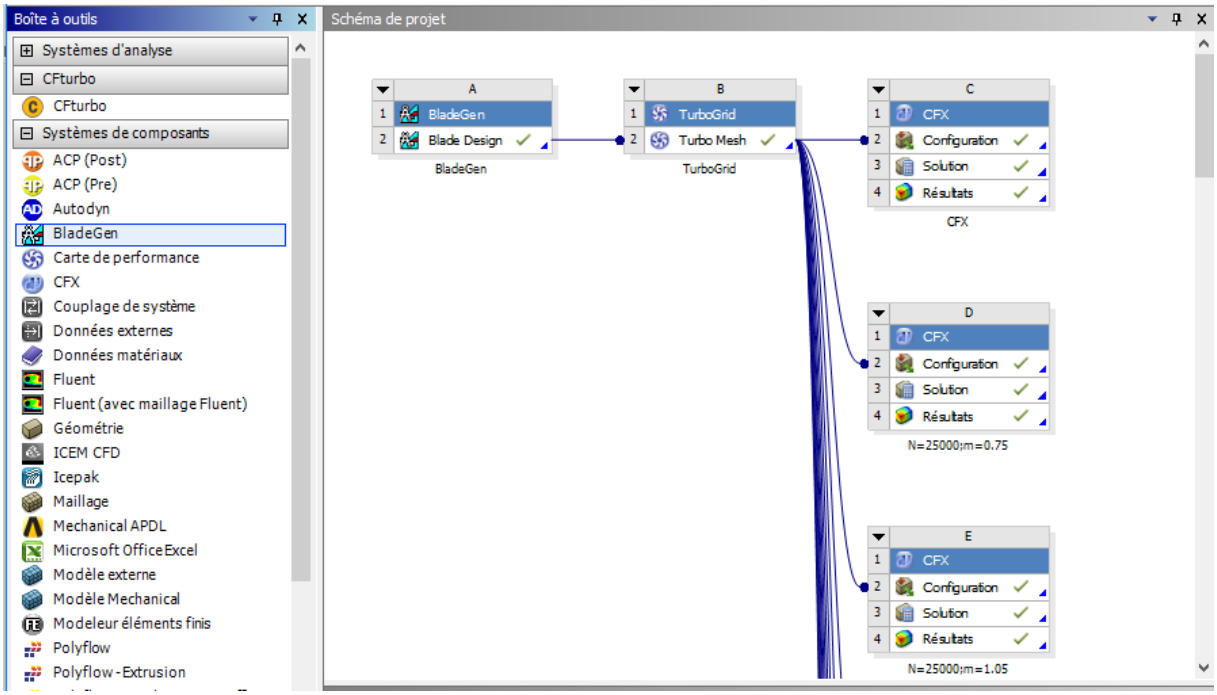

Figure3.1:ANSYS CFX workbench 19.0 interface

3.2.1.1 Design of the WHEEL:

The design of the geometry of the centrifugal compressor impeller, takes place in fourstages, as shown below on the images of the ANSYS Turbo Gen software interface for the design of parts

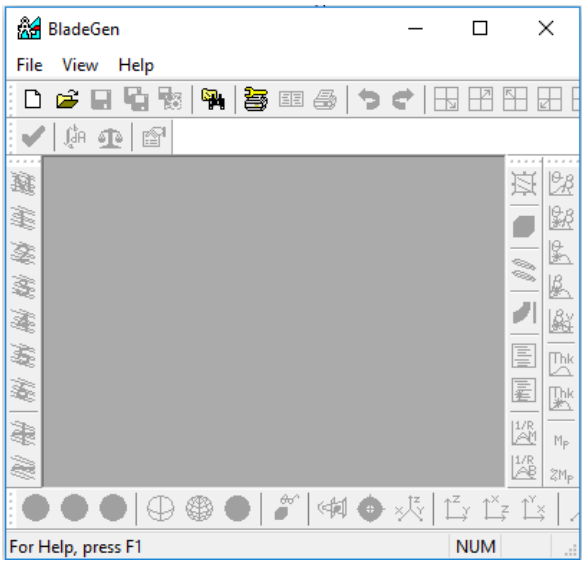

Figure 3.2: newblade gen file

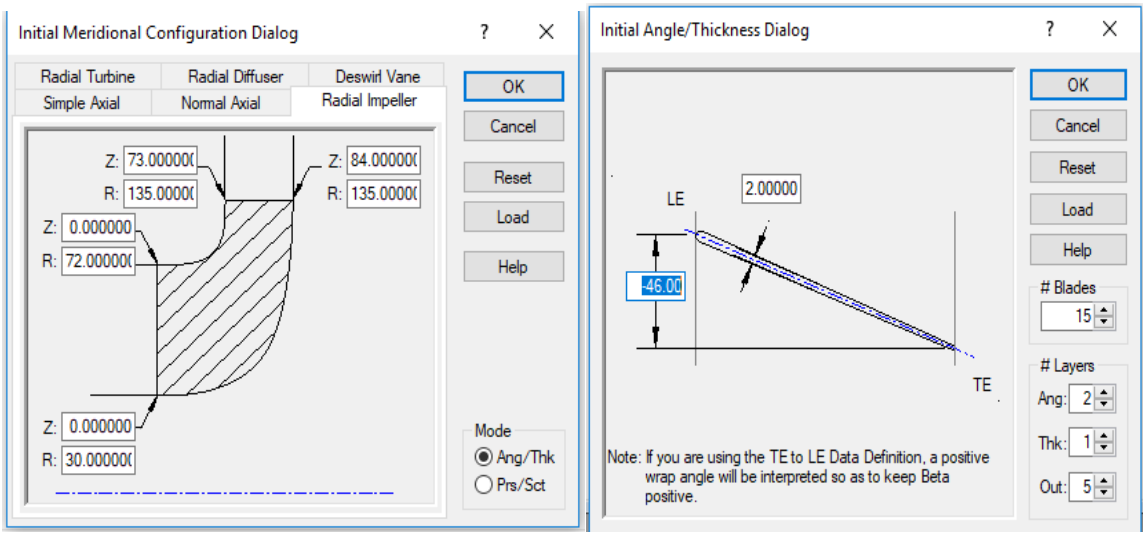

Figure 3.3: creation of blade geometry

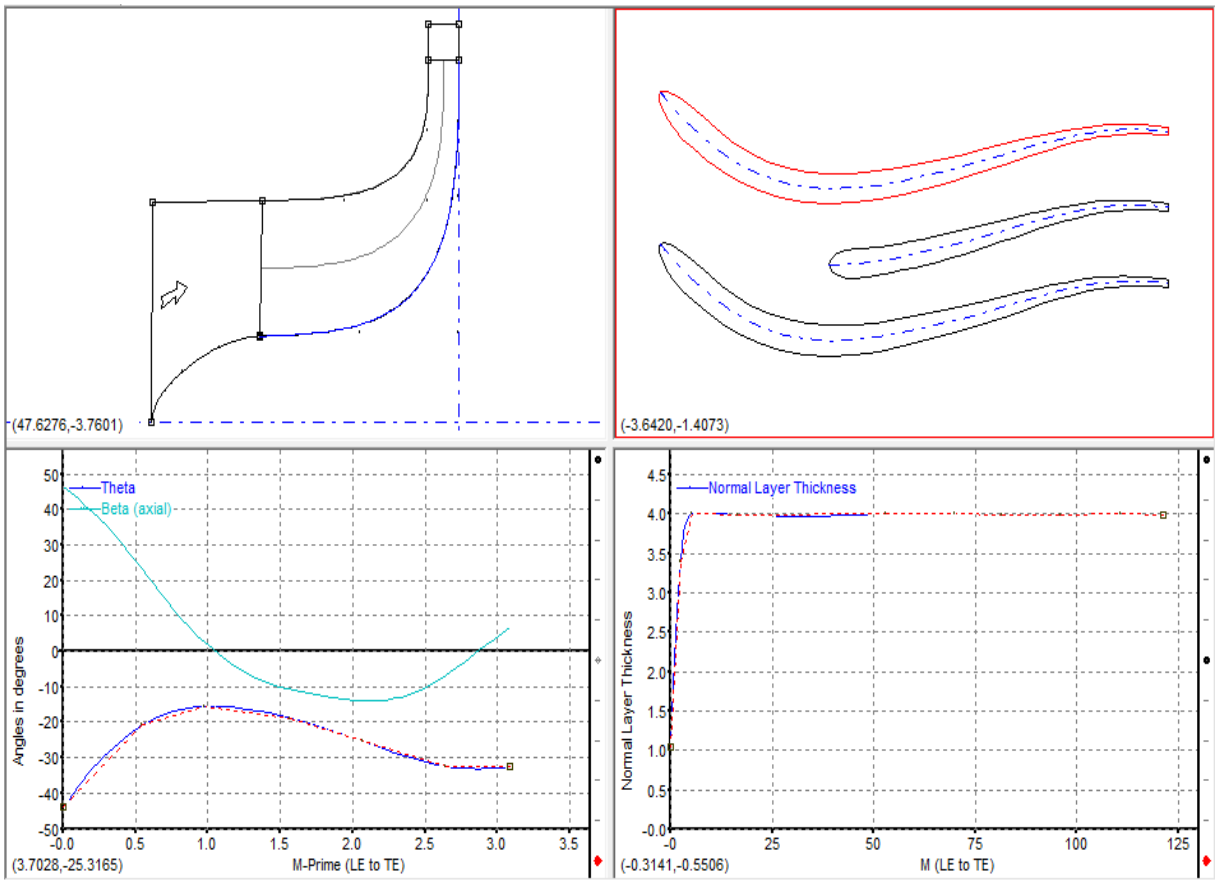

Figure 3.4: Presentation of the steps for the design of an impeller and diffuser by Gen V-11

- **First step :**

The design of the meridian vein by a predefined model and specific to the radial wheels, the surfaces of the hubs and the housings.

The surfaces are defined by two curves in the plane (z; r) where z and r arerespectively the axial and radial directions.

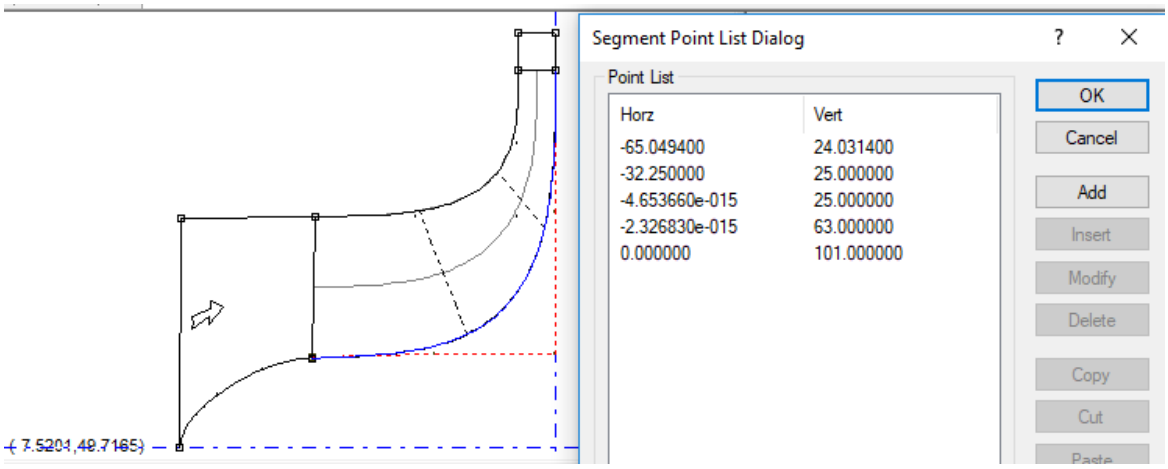

Figure 3.5:hub coordinates

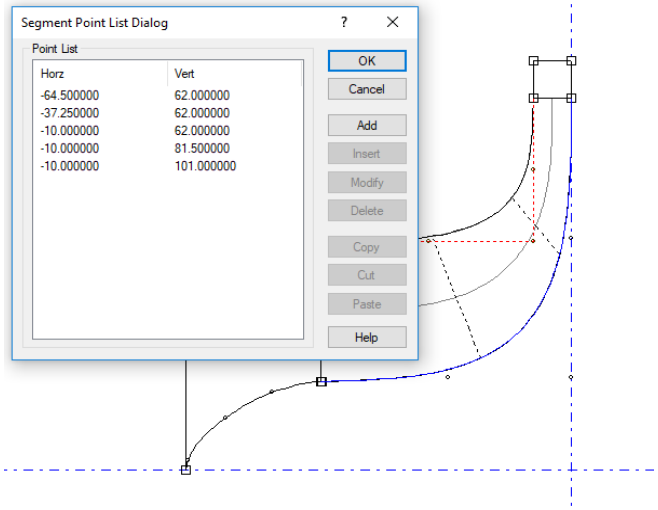

Figure 3.6: shroud coordinates

- **Second step:**

Consists of defining the wedging angles β and the overlap angle θ infunction of the meridian distance using a conformal transformation ofcoordinates of the reference R(x,y,z)n the reference R(M', θ) The equation to determinethe new coordinates is given by:

$$\delta M = \sqrt{\delta R \cdot \delta R + \delta Z \cdot \delta Z}$$

or:

M: Meridian distance

R: Radius

Z: Axial position

M': This is the meridian distance as a function of Ray:

$$\delta M' = \frac{\delta M}{R}$$

The angleθ: given by the following equation:

$$\delta\theta = \tan(\beta) \cdot \delta M'$$

In figures show both the wedging angle and overlap angle

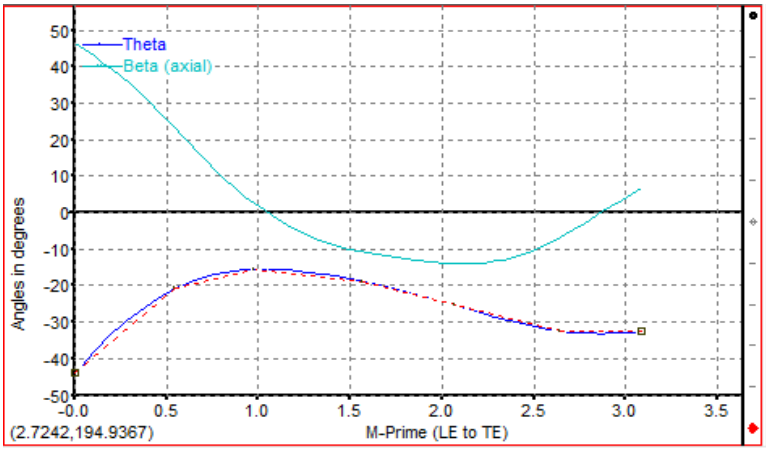

Figure 3.7: wedging and overlap angle of the blade

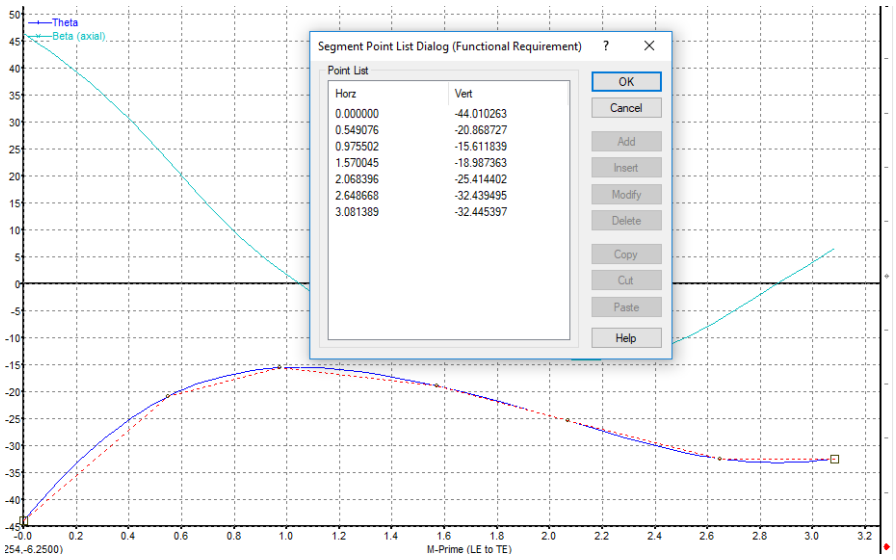

Figure 3.8:coordinates of wedging and overlap angle

- **Third step**

Consists of defining the thickness of the blade according to the meridian distance.

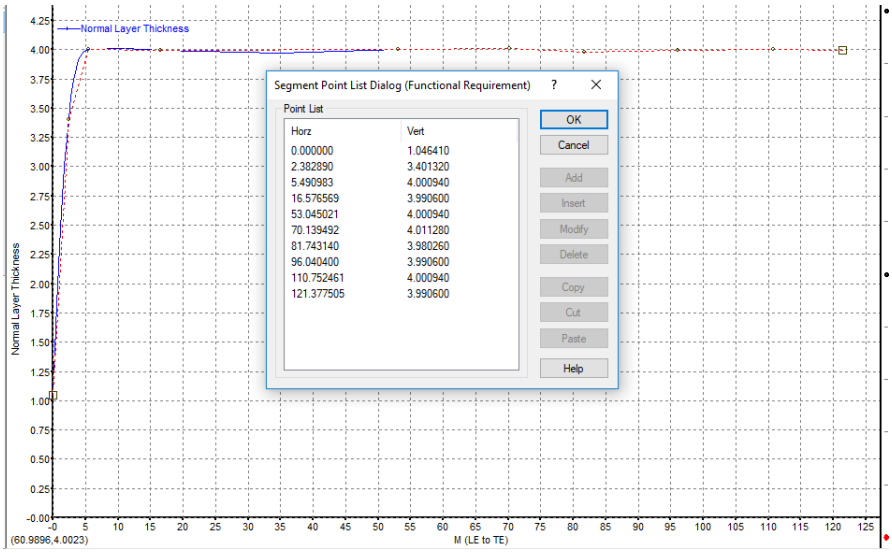

Figure 3.9: coordinates of blade thikness

- **Fourth step**

Consists of creating the geometric shape in three dimensions (3D) seefollowing figures:

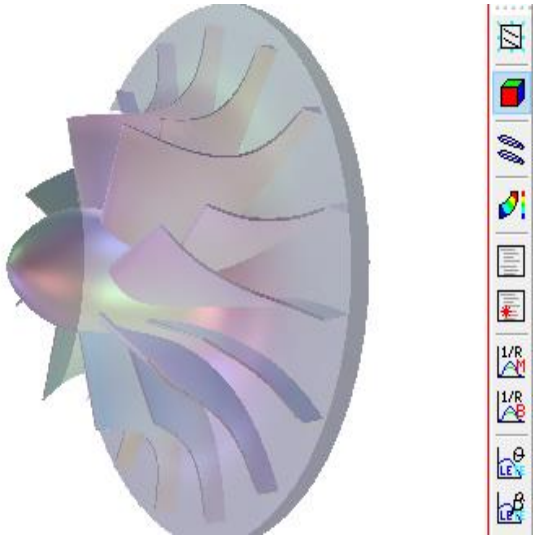

Figure 3.10:three dimensional view of impeller

- **Blade Splitter**

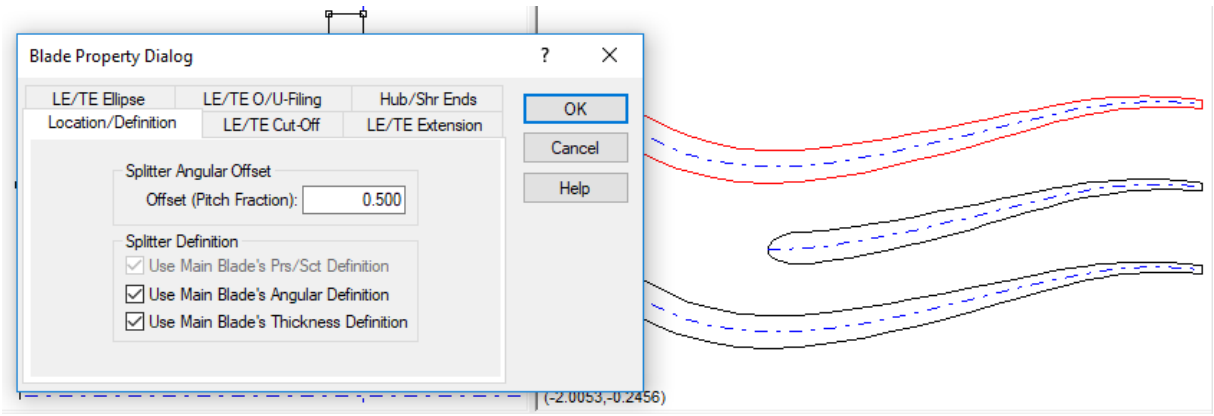

Figure 3.11:creation of splitter blades

3.2. 2.ANSYS CFX –Turbo Grid V-11:

This tool is used to generate a structured mesh suitable for applications fordifferent types of machines. But there is no precise rule to obtain agood mesh quality for certain shapes of complex geometries such as the wheelof the centrifugal compressor.The mesh of a structure is easier to generate using multi-block geometry;this technique consists of dividing the calculation domains into several compartments ofsimple geometric shapes and meshed them separately.

- **advantages:**

- Economical in number of elements and reduces the risk of numerical errors.

- **disadvantages:**

- In the case of a complex geometry such as the wheel of the centrifugal compressorthe mesh by this technique is not only difficult to generate but also itsquality can be bad.

in what follows, the different steps followed to generate the mesh.

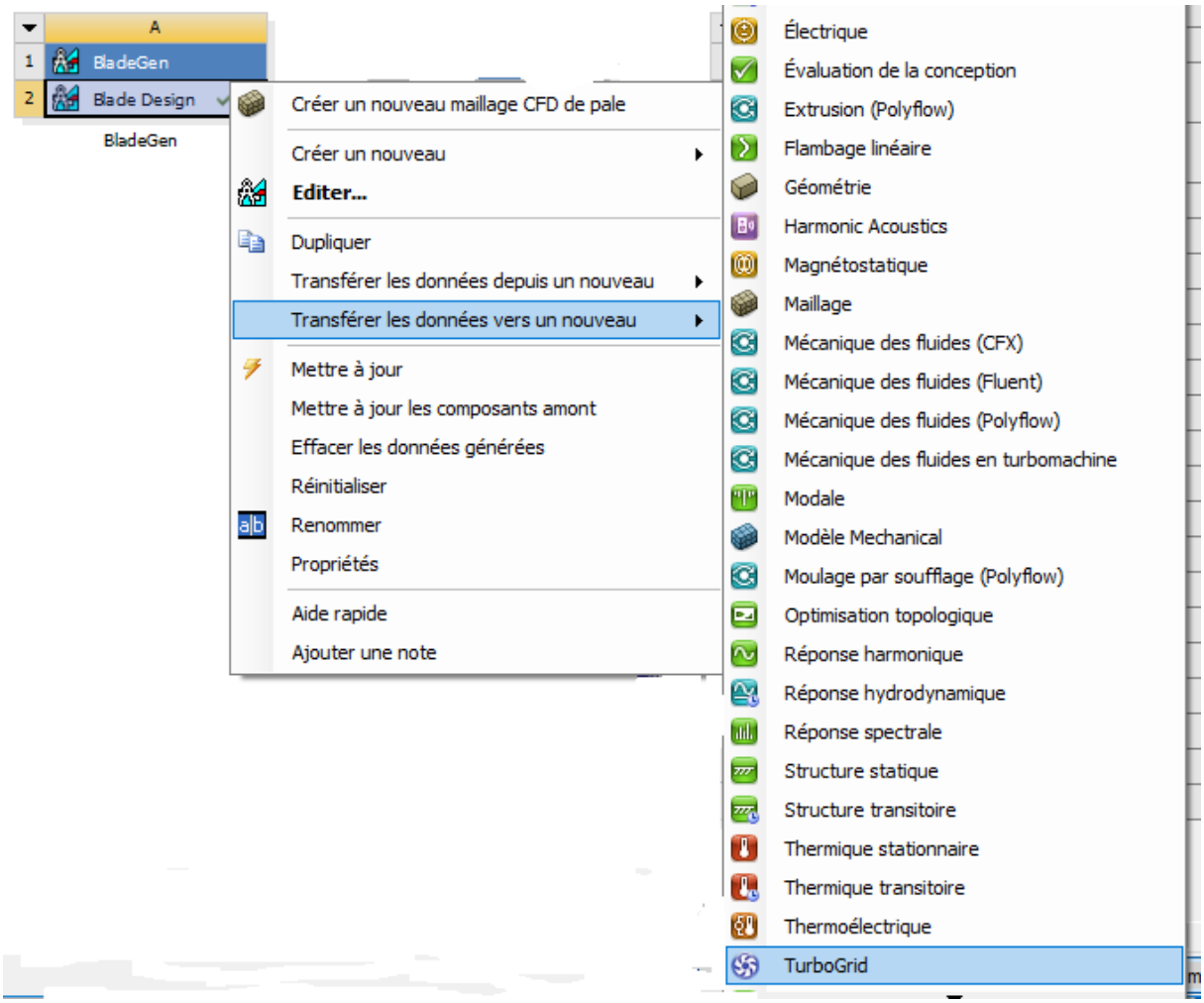

Figure 3.12:geometry exportation toTurboGrid**.**

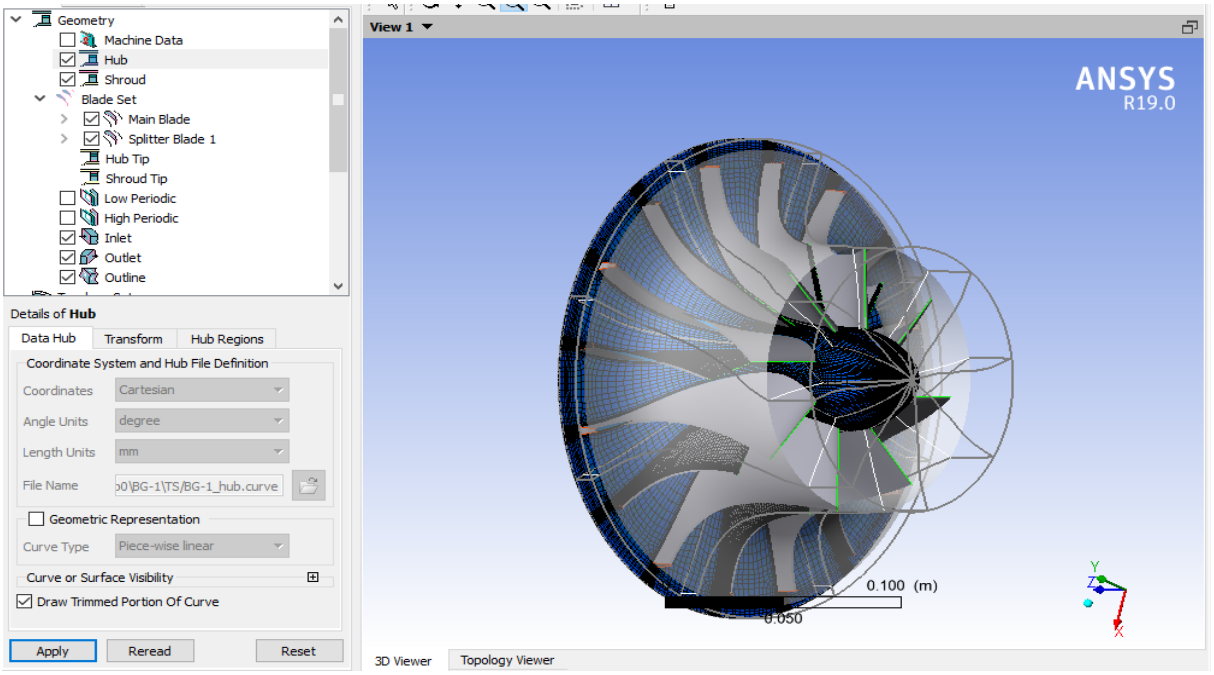

Figure 3.12: TurboGrid interface

Thickness between casing and a vane:

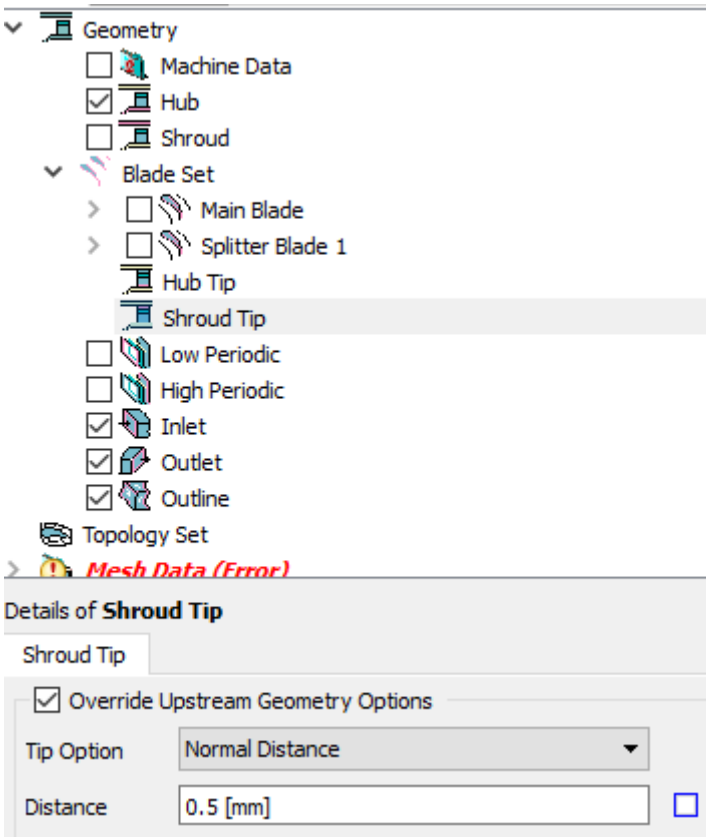

Figure 3.13: Thickness between casing and a vane

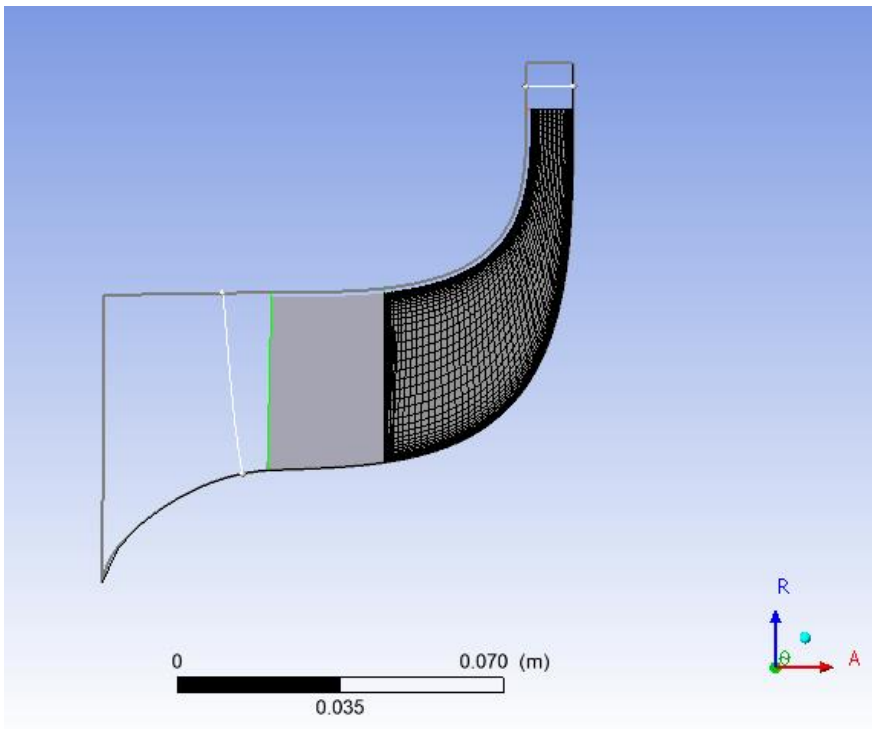

Figure 3.14: 2D blade mesh

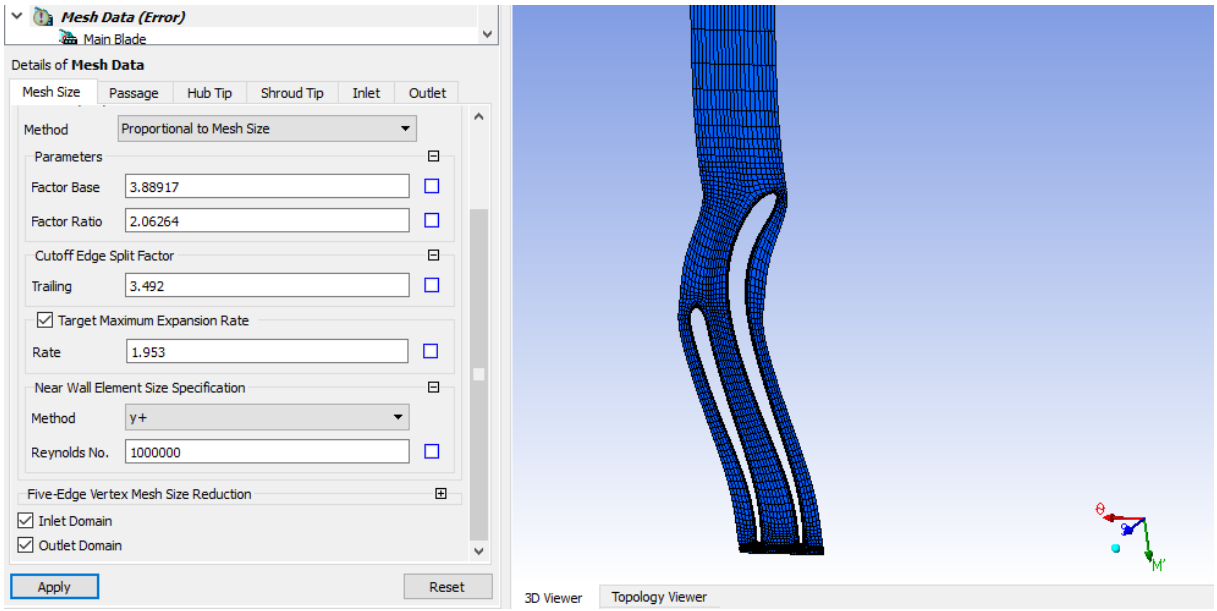

Figure 3.15:mesh factors

Mesh statistics and number of elements:

The mesh for a turbomachine depends on the following conditions:

- Maximum face angle: this is the largest angle of all the touching faces the knot, it measures the distortion. The value of this angle is 165.
- Minimum face angle: this is the smallest angle between two edges touching the node, the value of this angle 15.
- Number of connectivities: this is the number of elements in connection with a node maximum value 12 and minimum value 0.
- Element ratio of a volume: this is the ratio of the large volume to the small volume associated with a node, this ratio is positive.
- Ratio of the length of the stop: this is the ratio of the distance of the long stops on the smallest of the same face, the maximum value 10.
- Minimum volume: this is the volume of the positive mesh to ensure that no negative volume does not exist in the fluid passage.

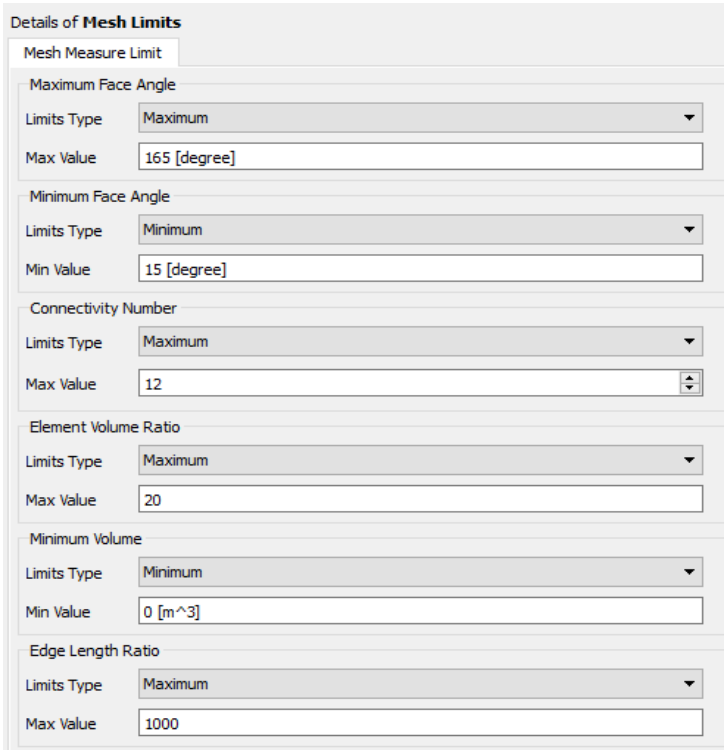

Figure 3.16:mesh limits

Note:

To obtain a very good quality mesh, the six conditions must bealready mentioned are met.The quality of a mesh grid directly affects the stability and accuracy ofcalculations, the better the mesh quality, the better the calculation result, the more preciseand more robust.

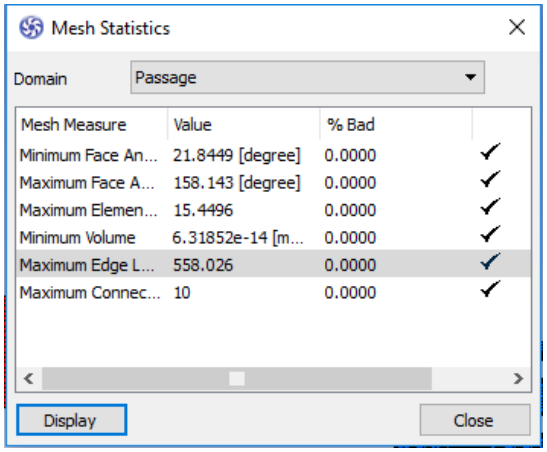

Figure 3.17: mesh statistics

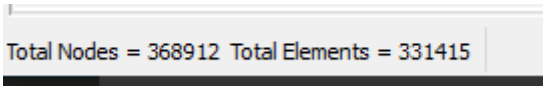

Figure 3.18: mesh nodes and elements

3.2.3.2.SolverAnsys CFX 19.0

In this module, we define the boundary and initial conditions corresponding to the flow regimes, then we choose the numerical scheme while fixing the number of iterations, as well as the convergence criterion and the nature of the fluid.

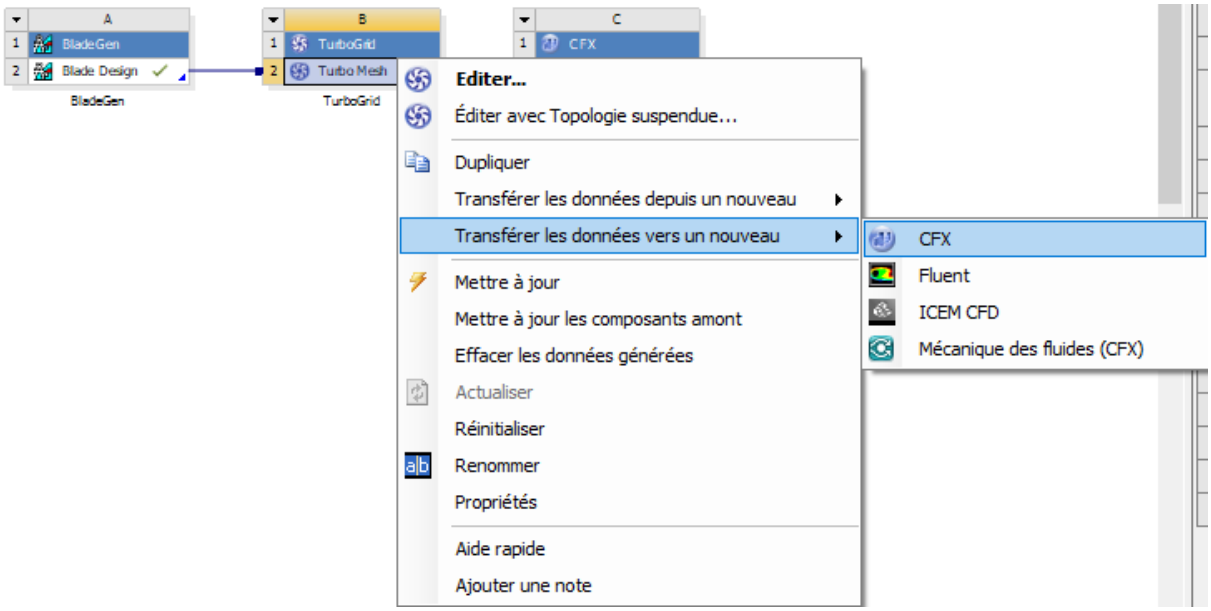

Figure 3.19: Data transfer to CFX

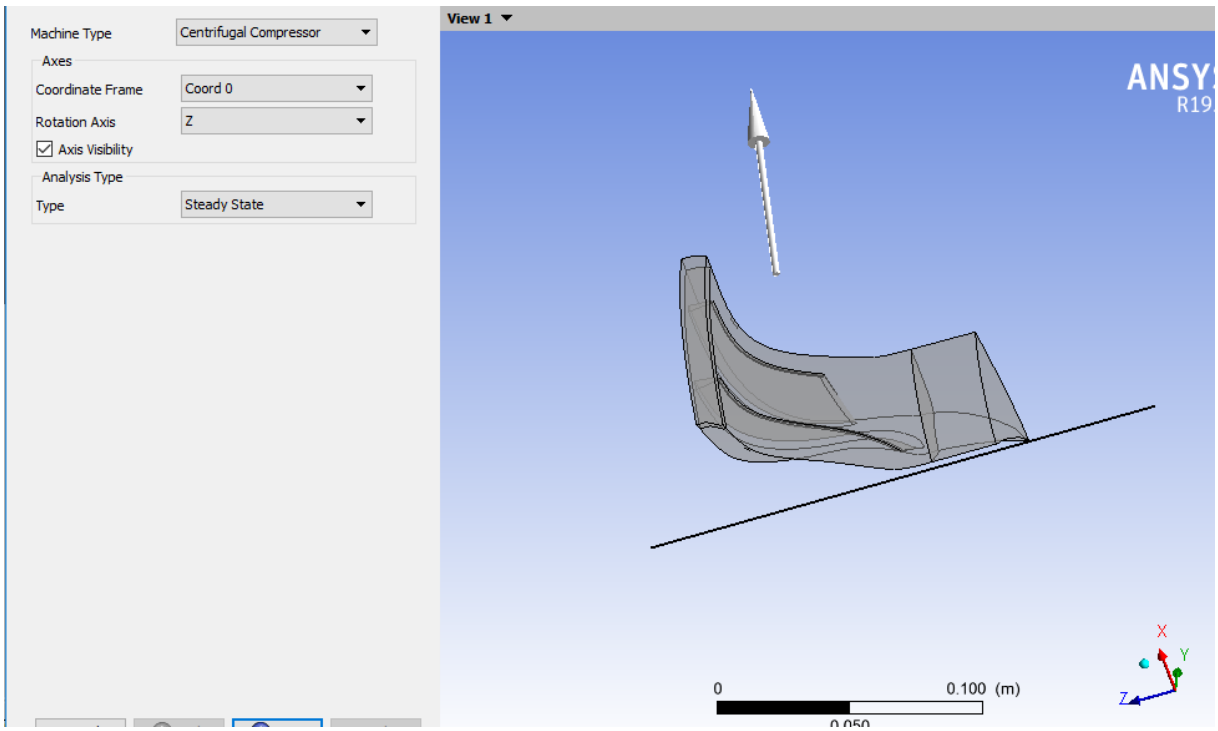

Figure 3.20:type of the machine determination

Boundary conditions:

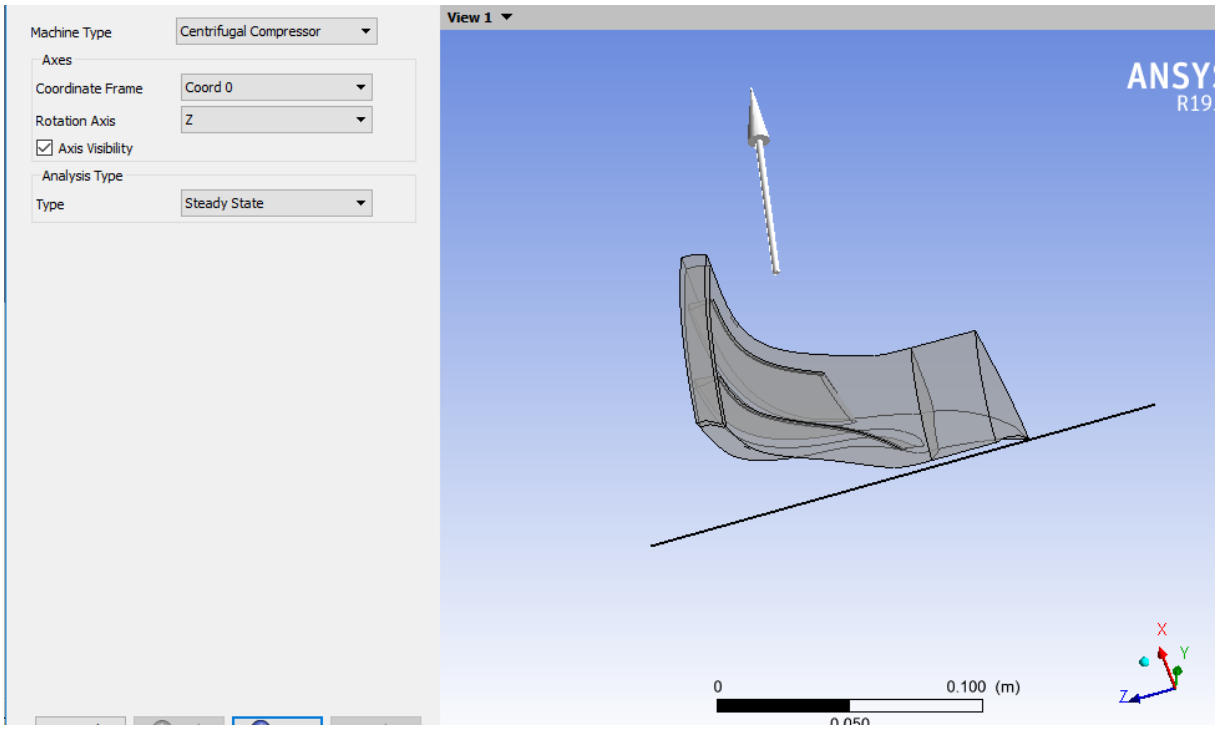

Figure 3.21:coordinate adjustment and axis of rotation

Solver Control

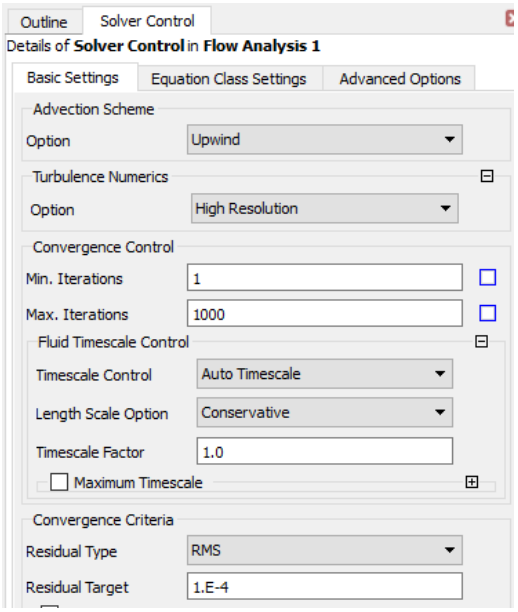

Figure 3.22 :solver control setting

The equations to solve are :

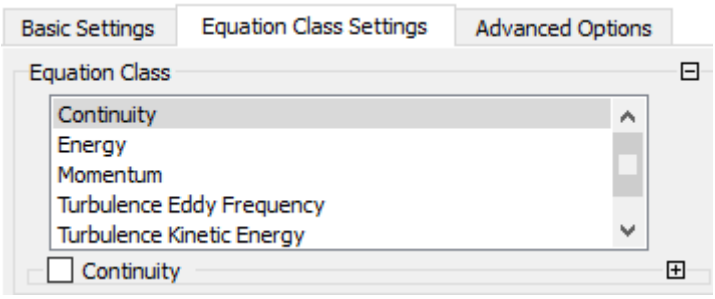

Figure 3.23: choice of equations to solve

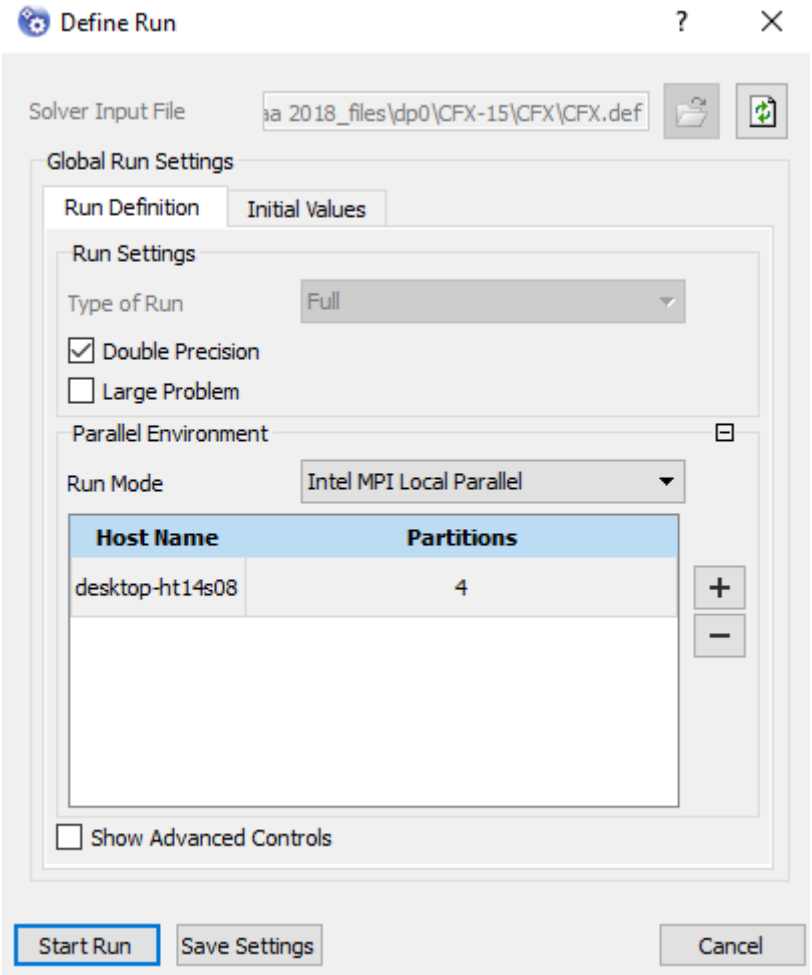

Figure 3.24: Global run setting

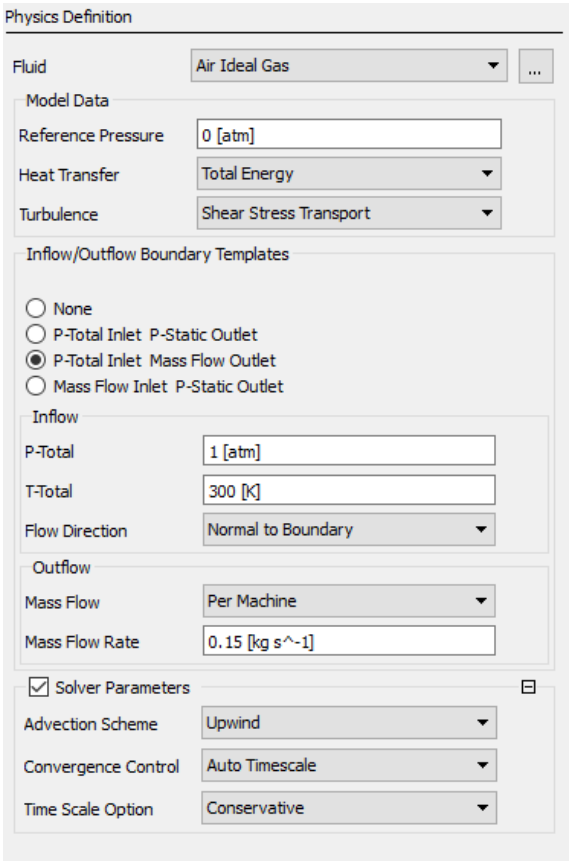

Figure 3.25: initial conditions

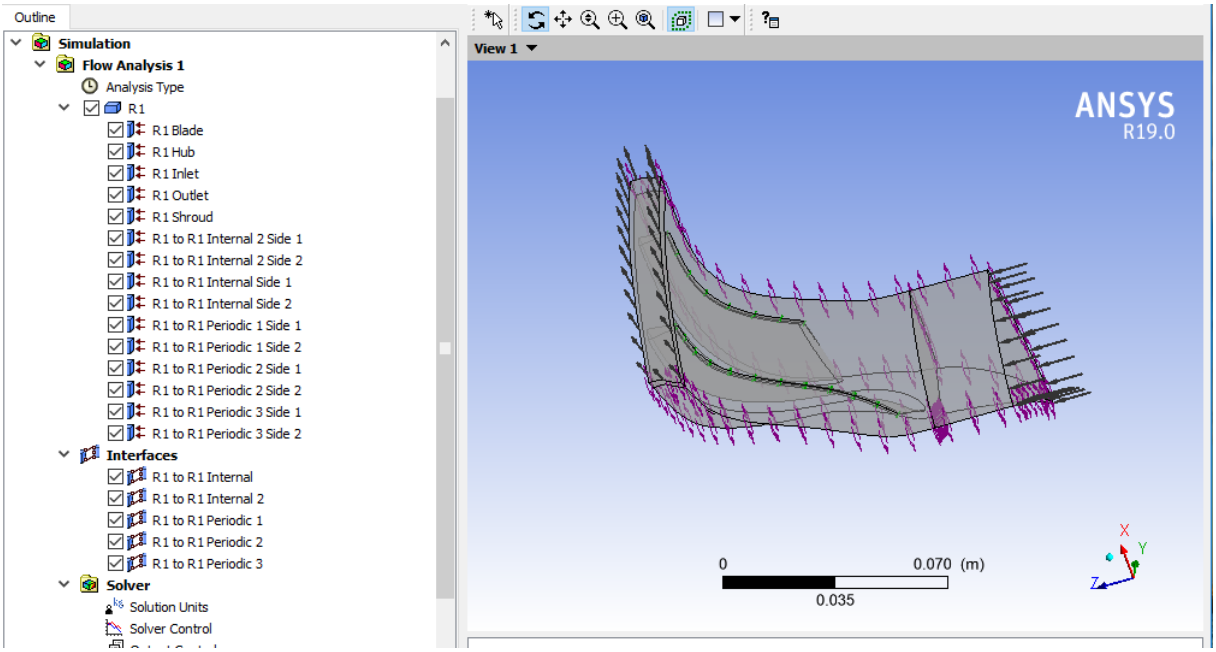

Figure 3.26:solver interface

CHAPTER 4

RESULTS AND DISCUSSION

4.1. Introduction

In this chapter we present the results obtained by the numerical simulation and by comparing with the experimental results for the centrifugal compressor wheel, and also to validate these results with other work done in the field of this subject.

In the first part of this chapter, we obtained the results by numerical simulation using the code ANSYS CFX for the impeller of the isolated compressor, and then analyze the aerothermodynamics parameters in nominal flow.

4.2. Mesh validation

In order to compare the experimental results with those of the numerical results obtained for the variation of the total pressure ratio for the three cases of given meshes, for a given rotational velocity N=15000rpm

Number of element / Mass Flow Rate	140756	193471	331415
0.2	1.32	1.29	1.247
0.3	1.29	1.27	1.239
0.4	1.26	1.25	1.235
0.5	1.25	1.25	1.231
0.6	1.25	1.23	1.230

Table 4.1: pressure ratio for different meshes and mass flow rate

The results obtained in the third case, where the number of elements is greater than the others, gave good results compared to the rest.

4.3.Presentation of the aerodynamic parameters for rotation speed N = 15000rpm and mass flow m = 0.4 kg / s:

4.3.1. Variation of pressure

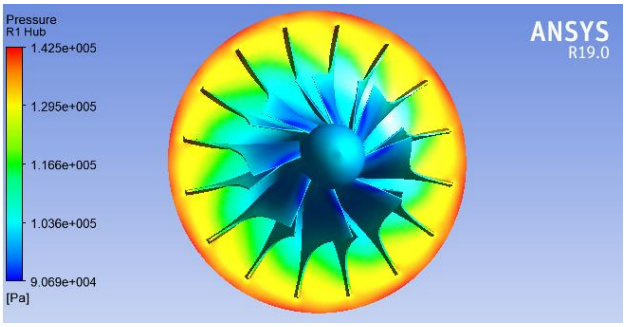

Figure 4.1: The pressure field on the wheel

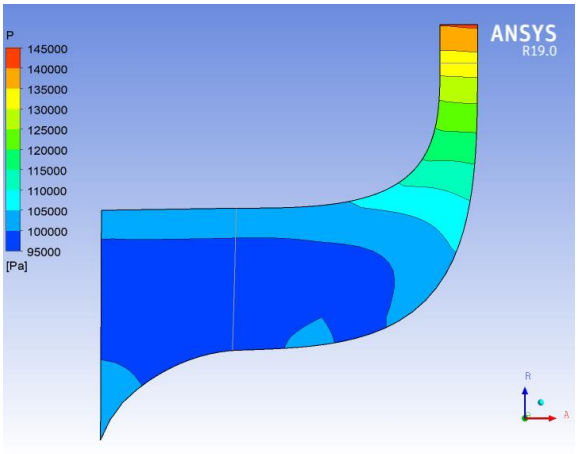

Figure 4.2: The contours of the static pressure on a meridian plane of the wheel.

According to the theoretical analysis given in Chapter I, we can geometrically divide the wheel into four zones:

- Zone "0": We observe negative values at the entry of the cone (depression) because of the effect of the rotation of the wheel, such that this effect creates zones of depression. But, in general the static pressure remains constant until the entry of the impeller, since there is no element which influences the fluid. Then, a regular increase in pressure to a maximum value at the outlet of the impeller, this increase corresponds to the shape of the passage section of the fluid and to the aerodynamic shape of the blades and also to the effect of rotation of wheel.
- Zone "1": At the entry of the wheel, the radius is small and the mean radius Rm of curvature tends to infinity since the flow is axial, this implies that the centrifugal force is important. So the pressure gradient is established from the hub to the housing.

- Zone “2”: In the middle of the channel (in the radial axial bend), the curvature in this plane is strong but it is finite, however the centrifugal force opposes that of the force due to the curvature but it is dominant . Thus, the pressure gradient from the housing to the hub is negative.
- Zone "3": At the exit of the wheel, the radius of curvature is almost equal to zero, therefore the curvature force is negligible and the centrifugal force becomes weak, since the mean radius Rm is large, therefore the pressure gradient is negative from the housing to the hub.

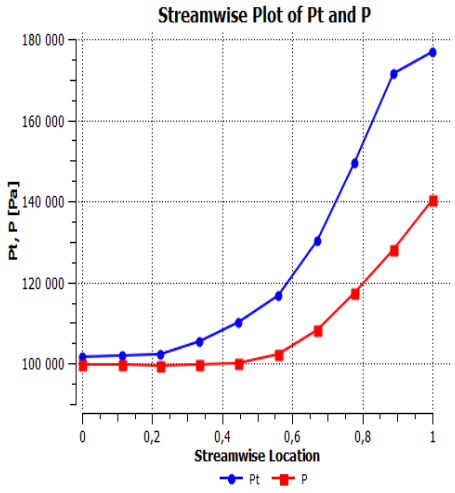

Figure 4.3: The variation of the static and total pressure in the wheel.

It can be split into two Z / Z0 rate intervals:

- When 0 <Z / Z0 <0.2: We observe no variation for the two pressures (static, total), since in this zone no obstacle can influence the movement of the fluid (work equals zero).
- When 0.2 <Z / Z0 <1: We observe an increase in the total and static pressure up to the exit of the impeller with maximum values of the pressure, in this zone the energy of the fluid will increase in the form of stop pressure.

This increase in total pressure, which is that of the stop pressure, will increase the static pressure and the kinetic energy of the fluid.

4.3.2. Variation of static and total temperature

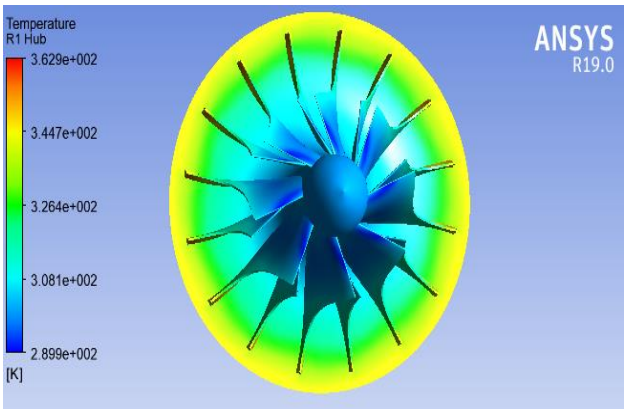

Figure 4.4: Temperature field on the wheel

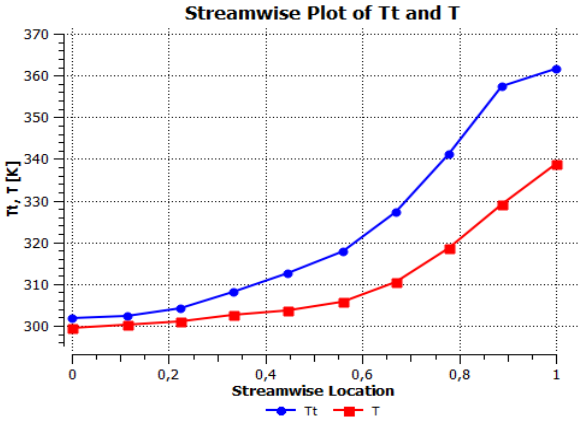

Figure 4.5: The variation of the static and total temperature in the wheel.

The curves given in figure 4.5 can be interpreted in two intervals:

- When 0 <Z / Z0 <0.2: We observe no variation for the two temperatures (static, total), since in this zone no element can have an effect on the movement of the fluid (the work equals zero).
- When 0.2<Z / Z0 <1: We observe an increase in the total and static temperature up to the exit of the impeller with maximum values of temperatures, in this zone the energy of the fluid will increase in the form of heat. .

Therefore, this increase in total temperature will increase the static temperature and kinetic energy of the fluid.

4.3.3. Mach number distribution

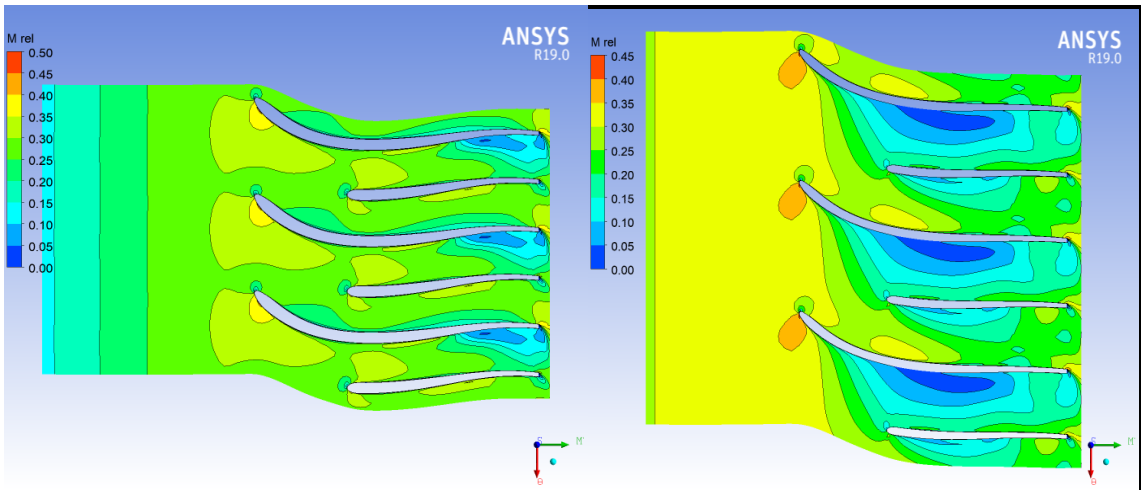

Figure 4.6: The variation of the relative Mach number in the vane-to-vane plane.

In figure 4.6, we give the evolution of the relative Mach number in the vane-to-vane plane. We observe, from this figure, that the relative Mach number remains constant until the entry of the wheel, since no parameter can influence the speed of the flow in the channel.

- In the intrados side with respect to the main and intermediate vanes, the flow of the fluid accelerates slightly then it becomes weak at the outlet of the impeller, this is due to the curvature of the surface of these vanes (decrease in tangential speed flow).
- in the extrados side the flow of the fluid flow decelerates until zones of low values of the relative Mach number are created, since a phenomenon of separation and recirculation of the fluid (this influences the tangential speed of the flow) and also the effect of the direction of rotation of the wheel.

4.3.4.Streamlines:

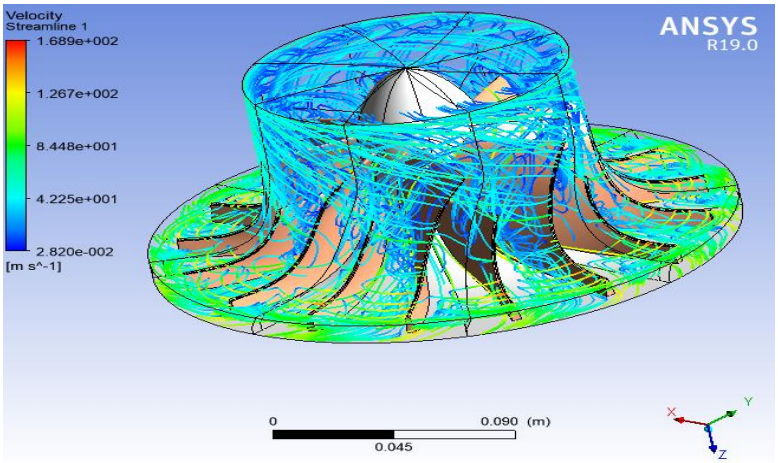

Figure 4.7: evolution of streamlines

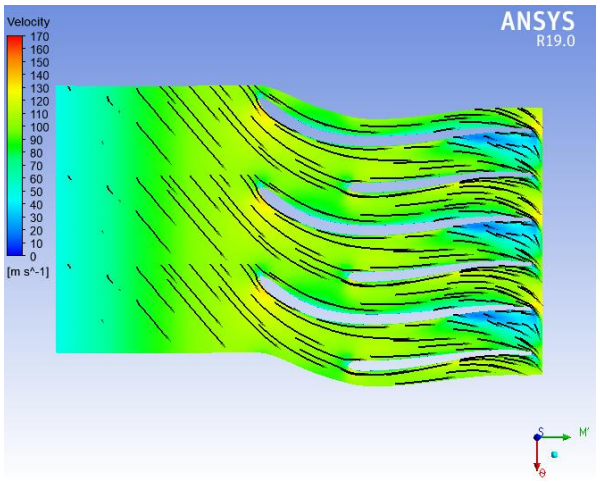

Figure 4.8 : The variation of speed in the blade-to-span plane compared to the 20% wingspan plane

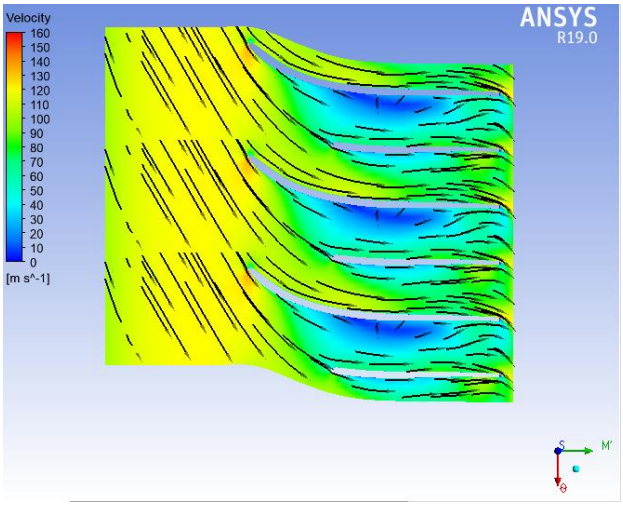

Figure 4.9 : The variation of speed in the blade-to-span plane compared to the 50% wingspan plane

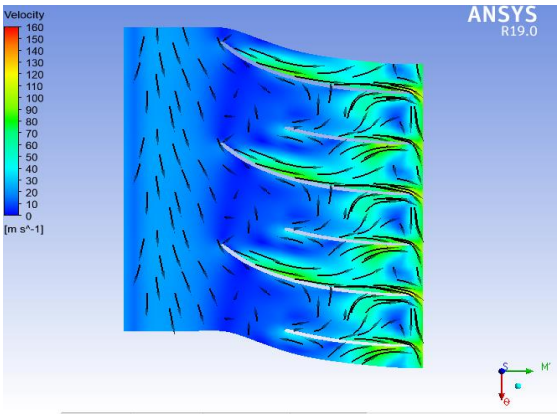

Figure 4.10: The variation of speed in the blade-to-span plane compared to the 80% wingspan plane

According to these figures, we observe an increase of the flow velocity at the extrados of the blades and a creation of small areas at the exit of the impeller with a low velocity in the plane at 20% (span). In the 50% span plane, the size of the low velocity zones becomes larger compared to the 20% span plane. Moreover, in the 80% span plane we observe an increase in velocity in the channel, but also at the inlet of the blades the direction of the fluid velocity flow is arbitrary and the speed at the outlet decreases.

Moreover, the creation of these zones for the three planes is due to the phenomena of recirculation, disbonding, interaction with the boundary layer, the effect of curvature of the blade surfaces and the direction of rotation of the impeller.

4.3.5. comparison table between compressor performance at different flow rates:

Compressor performance **m=0.4[kg/s]**	Compressor performance**m=0.2[kg/s]**
Rotation Speed=-2617.9900[radian s^-1]	Rotation Speed=-1570.8000 [radian s^-1]
Mass Flow Rate=0.4274[kg s^-1]	Mass Flow Rate=0.2041[kg s^-1]
Inlet Volume Flow Rate=0.3634[m^3 s^-1]	Inlet Volume Flow Rate=0.1732[m^3 s^-1]
Input Power=26517.2000[W]	Input Power=4623.1600[W]
Reference Radius=0.1008[m]	Reference Radius=0.1008[m]
Inlet Flow Coefficient= 0.0339	Inlet Flow Coefficient= 0.0269
Exit Flow Coefficient =0.2052	Exit Flow Coefficient =0.1897
Head Coefficient=3.5935	Head Coefficient=3.6723
Work Input Coefficient=0.8909	Work Input Coefficient= 0.9035
Total Pressure Ratio=1.7451	Total Pressure Ratio=1.2402
Total Temperature Ratio=1.2059	Total Temperature Ratio=1.0752
Total IsentropicEfficiency %=84.0303	Total Isentropic Efficiency %=84.6141
Total PolytropicEfficiency %=85.2339	Total Polytropic Efficiency %=85.0780

Table 4.1:comparison between compressor performance for m=0.4[kg/s] and m=0.2[kg/s]

4.3.5 Variation of the entropy S:

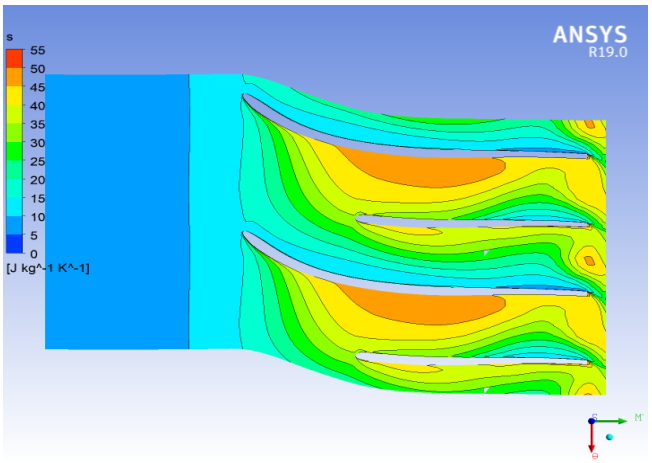

Figure 4.11: The variation of entropy (S) in vane-to-vane planes

In the figure, the entropy values in the extrados side of the main and spacer blades are higher, because the zones of disbonding and recirculation of the flow. In addition, the entropy values increases because the interaction of the flow between the impeller and the casing is greater and the disbonding zones are created. The entropy represents the energy losses in the impeller.

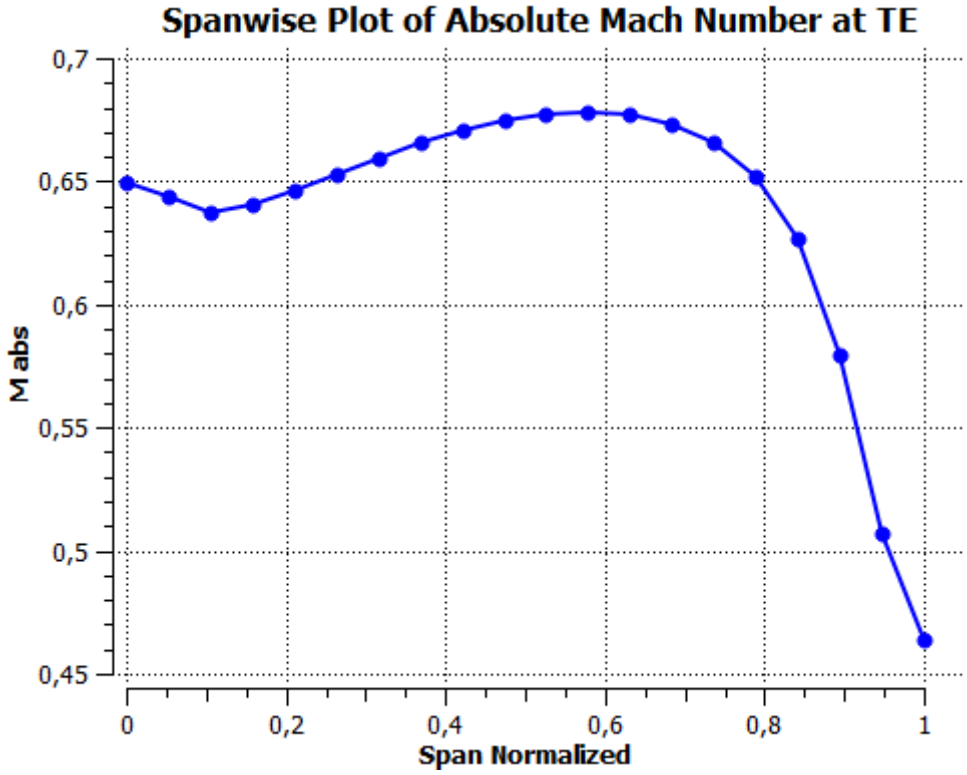

Figure 4.12: The variation of the absolute Mach number at the exit of the wheel

From this figure, we notice that the air flow curve($\dot{m}$ = 0.4 kg / s) at the level of the region very close to the hub and in the interval [0.8 - 1] of the ratio b / b0, the number of absolute Mach increases rapidly to a maximum value of 0.675 then it decreases slightly in the vicinity of the crankcase until the value of 0.46.

It should be noted that the maximum value of the absolute Mach number corresponds to the wake phenomenon, as well as its minimum number corresponds to the jet phenomenon.

4.4.Influence of mass flow on static pressure

4.4.1. Influence of mass flow on static pressure:

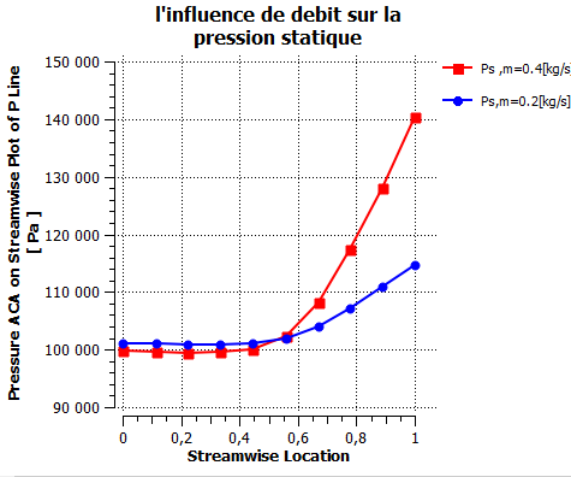

Figure 4.13: influence of the variation of the mass flow on static pressure

The figure 4.13 shows the variation of the static pressure in the impeller for two different air flow rates, $\dot{m}$ = 0.2 and 0.4kg / s.

The curves in this figure are interpreted as follows:

- In the interval 0 <Z / Z0 <0.5: We observe no variation of the static pressure and that when increasing the air flow the pressure decreases, since no element can have influence on the flow for the different air flow rates.
- In the interval 0.5<Z / Z0 <1: We observe an increase in the static pressure which will reach maximum values at the exit of the wheel, since there is an energy transfer between the wheel and the movement of the fluid.

4.4.2. Influence of mass flow onTotal pressure:

Figure 4.14 shows the variation of the total pressure in the impeller for different air flows $\dot{m}$ = 0.2 and 0.4 kg / s.

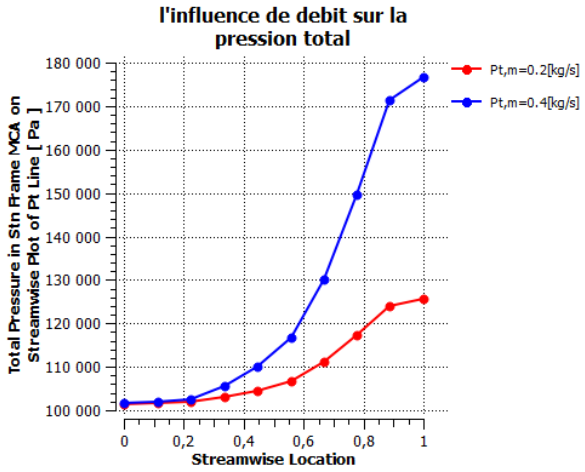

Figure 4.14: The influence of the air flow on the total pressure in the impeller.

This figure whose curves can be interpreted in two parts:

- When 0 <Z / Z0 <0.2: We can notice no variation in the total pressure, since nothing can influence the flow for the different air flows.
- When 0.2<Z / Z0 <1: We observe an increase in the total pressure to reach maximum values at the exit of the impeller, since there is an energy transfer between the impeller and the movement of the fluid. According to the curves, the total pressure varies proportionally with the air flow, but it is inversely proportional when the air flow becomes maximum.

4.4.3.influence of mass flow on statique temperature:

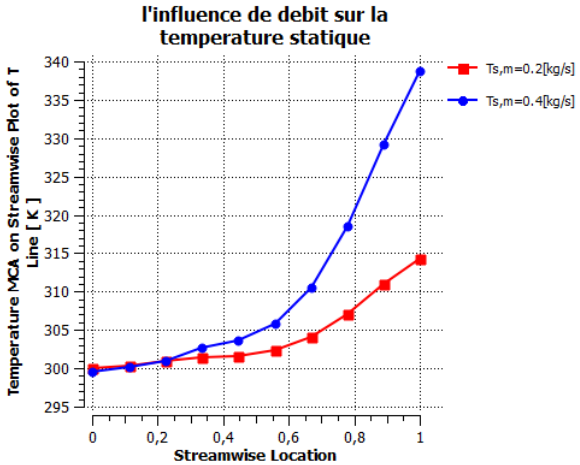

Figure 4.15: shows the static temperature variation in the impeller for different air flow rates,ṁ =0.2 and 0.4 kg/s

The curves of this figure, we notice :

- In the interval 0< Z/Z0 <0.2: No variation of the static temperature, and that when the airflow is increased the temperature becomes very low, because no element influences the flow at different airflows.
- In the range 0.2< Z/Z0 <1: An increase in the static temperature that will reach maximum values at the outlet of the impeller, since there is an energy transfer between the impeller and the fluid movement. Moreover, according to the curves in this figure, the temperature is inversely proportional with the variation of the air flow rate, it is maximum for an air flow rate of 0.2 kg/s and it is minimum for an air flow rate of 0.4kg/s.

4.4.4.Influenceof mass flow on total temperature:

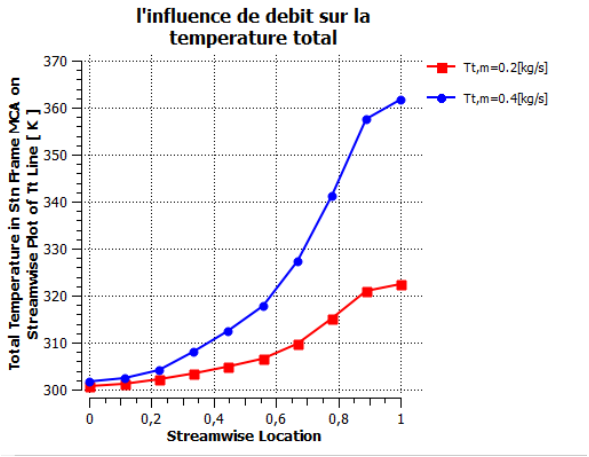

Figure 4.16:shows the total temperature variation in the impeller for different air flow rates,ṁ =0.2 and 0.4 kg/s.

From the curves of this figure, we notice:

- In the interval 0< Z/Z0 <0.2: We observe no variation in the total temperature and that when the airflow is increased the temperature becomes very low, this explains why no element influences the flow at different airflows.
- In the interval 0.2 < Z/Z0 <1: We notice a total temperature increase that will reach maximum values at the outlet of the impeller, since there is an energy transfer between the impeller and the fluid movement.

4.5.1Influenceof the speed of rotation on static and total pressure:

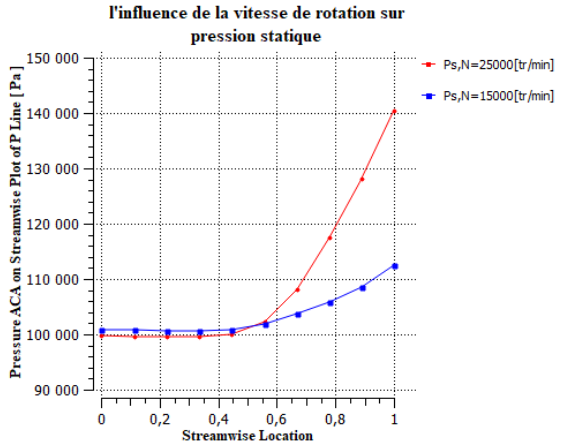

Figure 4.17: the static pressure variation in the impeller for different speeds

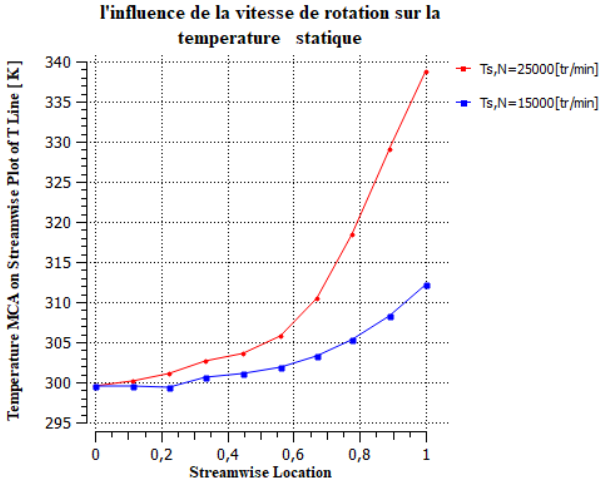

Figure 4.18: the static pressure variation in the impeller for different speeds

Figures 4.16 and 4.17 show the distribution of the static and total pressure on the blades for an air flow $\dot{m} = 0.4kg / s$ and for two rotation speeds 15000rpm and 20,000rpm

From these figures, we notice that the distribution of the static and total pressure for the main and intermediate vanes, takes a higher distribution profile in the case where the rotation speed is 20,000 rpm compared to that equal to 15,000 rpm.

4.5.2 Influenceof Wall function Y plus :

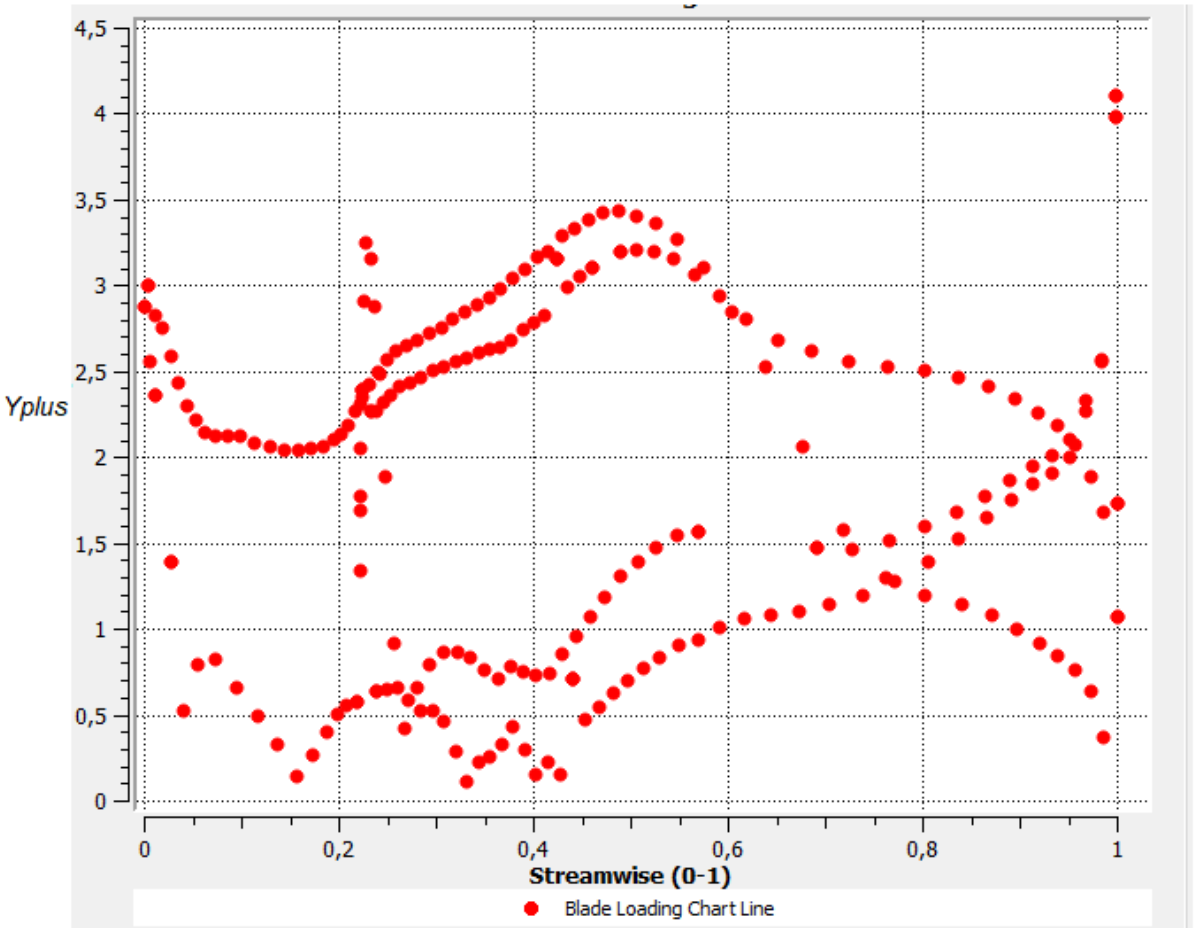

Figure 4.19: the curve of Yplus around the wheel

For the k-ω-SST model, the value of Y+ must not exceed the value of 5, in our case the Yplus vary between 0 and 3.5 which is less than 5 so the Y+ won't influence our results which conclude that the simulation is validated

CONCLUSION

The analysis of the flow in the centrifugal compressor wheel was carried out within the framework of this study using numerical techniques.

The numerical modeling of the three-dimensional, compressible, viscous and turbulent flow in stationary state in the stage was carried out by the calculation code ANSYS CFX. The numerical results obtained are comparable with the experimental results.

Before performing a simulation of the compressor wheel, the mesh is validated.

turbulence model with two transport equations used for the flow analysis and the determination of the performance in the centrifugal compressor impeller is the K-W S.S.T model.

Comparison with the results of the numerical characteristics described by the stationary turbulence model simulation reveals a better capability of the S.S.T turbulence model to describe the overall performance of the compressor.

In the centrifugal impeller at the nominal flow rate the analysis of the aerothermodynamic parameters have been determined, there is an increase of pressures, temperatures (total, static) up to maximum values at the outlet of the impeller, due to the increase of the fluid energy, which generates positive work.

For the distribution of the static pressure on the blades (main and spacer blades), we have noticed that a depression is created on the underside (PS), due to the shape of the blade surfaces and the effect of the direction of rotation of the impeller.

The speed and the relative Mach number decrease on the radar side (PS) since there is the creation of phenomena that affect the flow (recirculation, disbonding and turbulence) and the maximum areas of entropy on the PS side where the losses are maximum.

The meridian velocity or Mach number (relative and absolute) is maximum which corresponds to the wake and jet zone, and that an increase in airflow in the wake zone takes place.

The influence of airflow and rotational speed on the overall performance, so that as the airflow increases the pressure ratios (total, static) decrease and the power output of the

impeller increases as well. The increase in rotational speed causes an increase in pressure ratios and power, but with the decrease in total isentropic efficiency since this depends on the total pressure ratio as well as the total temperature ratio.

OUTLOOK

We hope for the continuation of this study to develop a new method for the dimensioning and analysis of the internal flow in the turbomachine.

Then, we will keep the same type of compressor impeller (centrifugal or axial) In addition, we will use the different numerical methods and LES turbulence models to improve the performance of the compressor wheel.

REFERENCES

[1] SIMULATION NUMERIQUE DE L'ECOULEMENT COMPRESSIBLE DANS L'ETAGE DU COMPRESSEUR CENTRIFUGE ,LAAZAB .S,2013,Blida

[2] DÉVELOPPEMENT D'UNE MÉTHODE DE SIMULATION DE POMPAGE AU SEIN D'UN COMPRESSEUR MULTI-ÉTAGÉ
MARTIAL DUMAS ,Montréal

[3] LA LIMITE DE POMPAGE DES COMPRESSEURS CENTRIFUGES.*TOUSSAINT Michel. Conservatoire National des Arts et Métiers LGPEES 292, rue Saint Martin 75141 PARIS 3ème*

[4] Guillaume. DUFOUR Analyse de l'écoulement tridimensionnel et instationnaire dans un compresseur centrifuge à fort taux de pression.2006

[3] Charlotte BARBIER Université des Sciences et Technologies de Lille 2002

[5] Simplified Adaptive Control of Centrifugal Compressors,Andrzej Tomasz Jerzak

[6] "ONERA écoulement secondaire compresseur centrifuge » 2003 www.onera.fr

[7] The finite difference method "Read Euler: he is our master in everything." Pierre-Simon Laplace (1749-1827) "

[8] Finite volume method in computational fluid dynamics,M.Darwish

[9] Governing Equations of Fluid Dynamics J.D. Anderson, Jr.

[10] **Wilcox, David C (1998)**. "Turbulence Modeling for CFD").

[11] direct numerical simulation of turbulent flows ,Giancarlo Alfonsi,ASME

[12] **Launder, B. E., and Sharma, B. I. (1974)**, "Application of the Energy Dissipation Model of Turbulence to the Calculation of Flow Near a Spinning Disc", Letters in Heat and Mass Transfer, vol. 1, no. 2, pp. 131-138.)

[13] (**Bardina, J.E., Huang, P.G., Coakley, T.J. (1997**Testing, and Development", NASA Technical Memorandum 110446.)

[14] International Journal of Heat and Fluid Flow

[15] Sharaf F. Al-Sharif
Center of Excellence in Desalination Technology, King Abdulaziz University, Jeddah
Saudi Arabi

[16] Extended integral wall-model for large-eddy simulations of compressible wall-bounded turbulent flows Jean-François Boussuge, Mathieu Catchirayer, J.-F Boussuge, Pierre Sagaut, Marc Montagnac, Xavier Garnaud, DimitriosPapadogiannis

[17]Turbomachinery: Design and Theory

[18]Rodi Journal of Hydraulic Engineering, 2017, 143(5)

[19] An Introduction to Turbulence Modeling for CFD Gerald Recktenwald;February 19, 2020

[20] AEA-Technology 2010 ,ansyscfx 12.1 documentation ,Version 12.1 ,Advanced Scientific Computing Ltd ,Wateroo ,CANADA